VYSOKÉ UČENÍ TECHNICKÉ V BRNĚ FAKULTA STROJNÍHO INŽENÝRSTVÍ

CEITEC
Central European Institute of Technology
BRNO | CZECH REPUBLIC

SOČ
středoškolská odborná činnost

Jak psát vědecké články?

Ing. Petr Dvořák, Ph.D.
petr.dvorak@ceitec.vutbr.cz

15. září 2023 Letní soustředění vítězů SOČ, Brno

SNPTM
SDRUŽENÍ NA PODPORU TALENTOVANÉ MLÁDEŽE ČR

0000-0003-3659-9249
RESEARCHER ID A-9810-2014

Ing. Petr Dvořák, Ph.D.

petr.dvorak@ceitec.vutbr.cz

Control and near-field detection of surface plasmon interference patterns P Dvořák, T Neuman, L Brinek, T Šamořil, R Kalousek, P Dub, ... Nano letters 13 (6), 2558-2563	62	2013
Ultrasmooth metallic foils for growth of high quality graphene by chemical vapor deposition P Procházka, J Mach, D Bischoff, Z Lišková, P Dvořák, M Vaňatka, ... Nanotechnology 25 (18), 185601	51	2014
Imaging of near-field interference patterns by aperture-type SNOM–influence of illumination wavelength and polarization state P Dvořák, Z Édes, M Kvapil, T Šamořil, F Ligmajer, M Hrtoň, R Kalousek, ... Optics Express 25 (14), 16560-16573	27	2017
High-resolution quantitative phase imaging of plasmonic metasurfaces with sensitivity down to a single nanoantenna P Bouchal, P Dvorak, J Babocky, Z Bouchal, F Ligmajer, M Hrton, ... Nano letters 19 (2), 1242-1250	26	2019
Quantitative 3D phase imaging of plasmonic metasurfaces J Babocky, A Krizova, L Strbkova, L Kejik, F Ligmajer, M Hrton, P Dvorak, ... ACS Photonics 4 (6), 1389-1397	20	2017
In-situ magnetic nano-patterning of Fe films grown on Cu (100) SS Zaman, P Dvořák, R Ritter, A Buchsbaum, D Stickler, HP Oepen, ... Journal of Applied Physics 110 (2)	19	2011
Invited article: direct phase mapping of broadband Laguerre-Gaussian metasurfaces A Faßbender, J Babocký, P Dvořák, V Křápek, S Linden APL Photonics 3 (11)	11	2018
Near-field digital holography: a tool for plasmon phase imaging P Dvořák, M Kvapil, P Bouchal, Z Édes, T Šamořil, M Hrtoň, F Ligmajer, ... Nanoscale 10, 21363-21368	11	2018
Patterning large area plasmonic nanostructures on nonconductive substrates using variable pressure electron beam lithography J Babocký, P Dvořák, F Ligmajer, M Hrtoň, T Šikola, J Bok, J Fiala Journal of Vacuum Science & Technology B 34 (6)	5	2016
Effect of deposition angle on fabrication of plasmonic gold nanocones and nanodiscs J Liška, F Ligmajer, L Kejík, M Kvapil, P Dvořák, M Horký, NS Leitner, ... Microelectronic Engineering 228, 111326	2	2020

Times Cited and Publications Over Time

DOWNLOAD

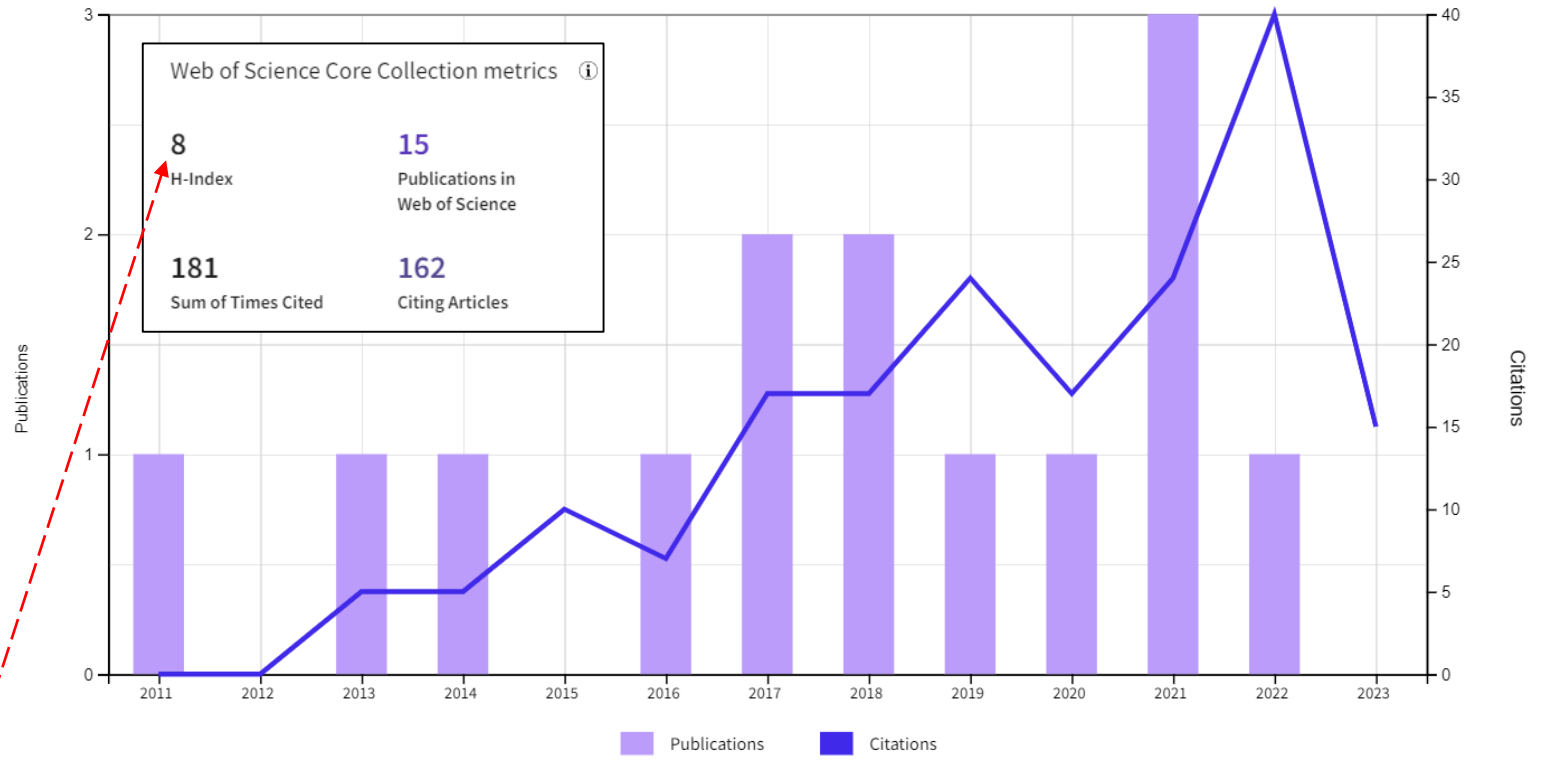

Vzorové (vysněné) žurnály

https://www.nature.com/

https://www.sciencemag.org/

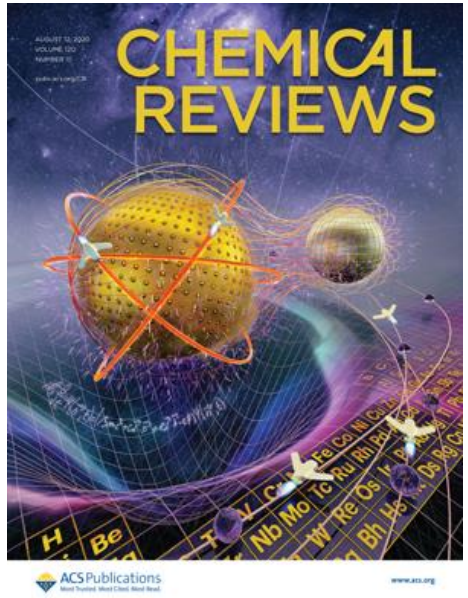

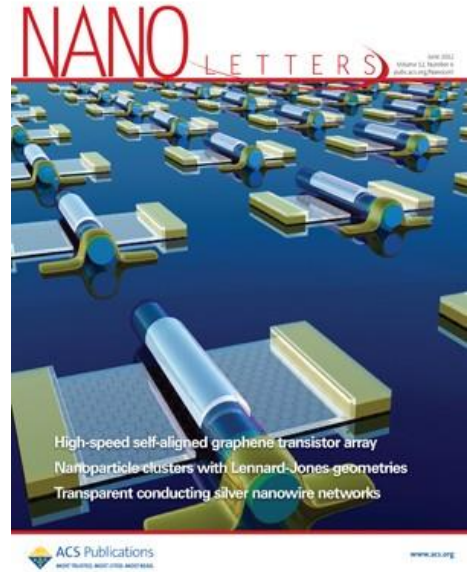

https://pubs.acs.org/

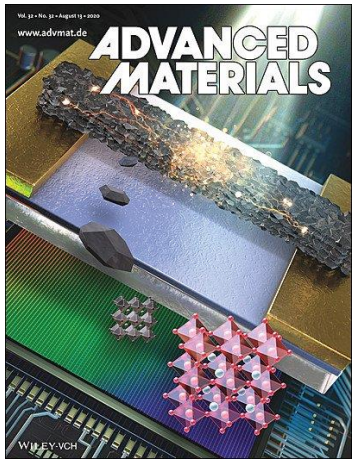

https://onlinelibrary.wiley.com/

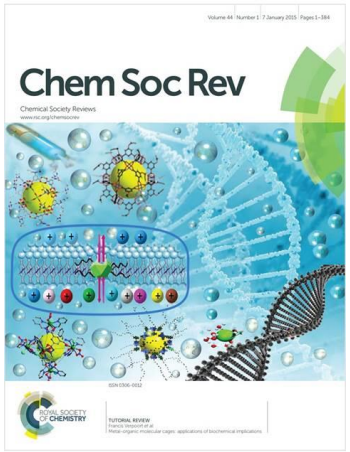

https://www.rsc.org/

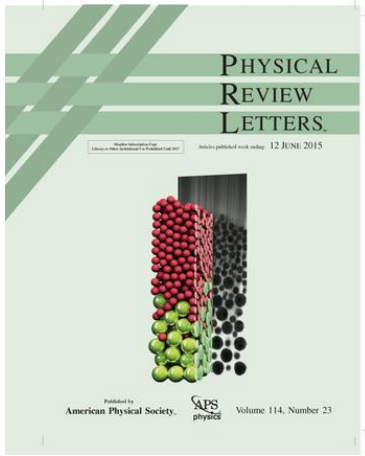

https://journals.aps.org/

https://www.journals.elsevier.com/

InCites Journal Citation Reports

peer-reviewed journals

Clarivate Analytics

Web of Science (*webofknowledge.com*)

Rank	Full Journal Title	Journal Impact Factor	Quartile
1	CA-A CANCER JOURNAL FOR CLINICIANS	292.278	Q1
2	NEW ENGLAND JOURNAL OF MEDICINE	74.699	Q1
3	Nature Reviews Materials	71.189	Q1
4	NATURE REVIEWS DRUG DISCOVERY	64.797	Q1
5	LANCET	60.392	Q1
6	WHO Technical Report Series	59.000	Q1
7	NATURE REVIEWS MOLECULAR CELL BIOLOGY	55.470	Q1
8	Nature Reviews Clinical Oncology	53.276	Q1
9	NATURE REVIEWS CANCER	53.030	Q1
10	CHEMICAL REVIEWS	52.758	Q1
11	Nature Energy	46.495	Q1
12	JAMA-JOURNAL OF THE AMERICAN MEDICAL ASSOCIATION	45.540	Q1
13	REVIEWS OF MODERN PHYSICS	45.037	Q1
14	CHEMICAL SOCIETY REVIEWS	42.846	Q1
15	NATURE	42.778	Q1
16	SCIENCE	41.845	Q1
17	Nature Reviews Disease Primers	40.689	Q1
18	World Psychiatry	40.595	Q1
20	NATURE REVIEWS IMMUNOLOGY	40.358	Q1
21	NATURE MATERIALS	38.663	Q1
22	CELL	38.637	Q1
23	NATURE BIOTECHNOLOGY	36.558	Q1
24	NATURE MEDICINE	36.130	Q1
25	Living Reviews in Relativity	35.429	Q1

Journal name	2022 JIF
CA-A CANCER JOURNAL FOR CLINICIANS	254.7
LANCET	168.9
NEW ENGLAND JOURNAL OF MEDICINE	158.5
JAMA-JOURNAL OF THE AMERICAN MEDICAL ASSOCIATION	120.7
NATURE REVIEWS DRUG DISCOVERY	120.1
NATURE REVIEWS DRUG DISCOVERY	120.1
NATURE REVIEWS MOLECULAR CELL BIOLOGY	112.7
BMJ-British Medical Journal	105.7
NATURE REVIEWS IMMUNOLOGY	100.3
NATURE REVIEWS MICROBIOLOGY	88.1
Nature Reviews Materials	83.5
Nature Reviews Materials	83.5
NATURE MEDICINE	82.9
NATURE MEDICINE	82.9
NATURE MEDICINE	82.9
Nature Reviews Disease Primers	81.5
Nature Reviews Clinical Oncology	78.8
NATURE REVIEWS CANCER	78.5
Lancet Respiratory Medicine	76.2
Lancet Respiratory Medicine	76.2
World Psychiatry	73.3
World Psychiatry	73.3
Nature Reviews Gastroenterology & Hepatology	65.1
NATURE	64.8
CELL	64.5
CELL	64.5
Lancet Psychiatry	64.3
Lancet Psychiatry	64.3
CHEMICAL REVIEWS	62.1
SCIENCE	56.9
Nature Energy	56.7
Nature Energy	56.7
LANCET INFECTIOUS DISEASES	56.3
LANCET ONCOLOGY	51.1
ANNALS OF ONCOLOGY	50.5
CANCER CELL	50.3
CANCER CELL	50.3
Lancet Public Health	50.0
Lancet Public Health	50.0
Nature Reviews Cardiology	49.6
LANCET NEUROLOGY	48.0
NATURE METHODS	48.0
NATURE BIOTECHNOLOGY	46.9
CHEMICAL SOCIETY REVIEWS	46.2
JOURNAL OF CLINICAL ONCOLOGY	45.3
Lancet Diabetes & Endocrinology	44.5
REVIEWS OF MODERN PHYSICS	44.1

Druhy a struktura článku

- Vědecký článek (**Article**) – 2000 až 5000 slov, 4-5 obrázků, strukturovaný
- Krátký článek (**Letter**) – do 2500 slov, max. 3 obrázky, volnější forma
- Přehledový článek (**Review**) – velké množství citací, autoři jsou kapacity v oboru
- Jiné (**Perspective**, **News & Comment**,…)

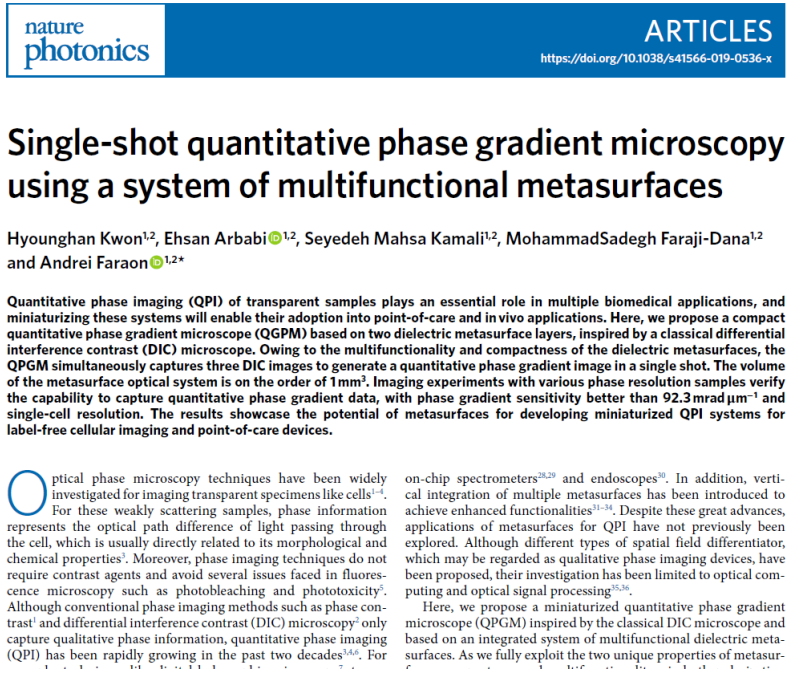

nature photonics
ARTICLES
https://doi.org/10.1038/s41566-019-0536-x

Single-shot quantitative phase gradient microscopy using a system of multifunctional metasurfaces

Hyounghan Kwon[1,2], Ehsan Arbabi[1,2], Seyedeh Mahsa Kamali[1,2], MohammadSadegh Faraji-Dana[1,2] and Andrei Faraon[1,2]*

Quantitative phase imaging (QPI) of transparent samples plays an essential role in multiple biomedical applications, and miniaturizing these systems will enable their adoption into point-of-care and in vivo applications. Here, we propose a compact quantitative phase gradient microscope (QGPM) based on two dielectric metasurface layers, inspired by a classical differential interference contrast (DIC) microscope. Owing to the multifunctionality and compactness of the dielectric metasurfaces, the QPGM simultaneously captures three DIC images to generate a quantitative phase gradient image in a single shot. The volume of the metasurface optical system is on the order of 1 mm³. Imaging experiments with various phase resolution samples verify the capability to capture quantitative phase gradient data, with phase gradient sensitivity better than 92.3 mrad μm⁻¹ and single-cell resolution. The results showcase the potential of metasurfaces for developing miniaturized QPI systems for label-free cellular imaging and point-of-care devices.

Optical phase microscopy techniques have been widely investigated for imaging transparent specimens like cells[1–4]. For these weakly scattering samples, phase information represents the optical path difference of light passing through the cell, which is usually directly related to its morphological and chemical properties[3]. Moreover, phase imaging techniques do not require contrast agents and avoid several issues faced in fluorescence microscopy such as photobleaching and phototoxicity[5]. Although conventional phase imaging methods such as phase contrast[1] and differential interference contrast (DIC) microscopy[2] only capture qualitative phase information, quantitative phase imaging (QPI) has been rapidly growing in the past two decades[3,4,6]. For

on-chip spectrometers[28,29] and endoscopes[30]. In addition, vertical integration of multiple metasurfaces has been introduced to achieve enhanced functionalities[31–34]. Despite these great advances, applications of metasurfaces for QPI have not previously been explored. Although different types of spatial field differentiator, which may be regarded as qualitative phase imaging devices, have been proposed, their investigation has been limited to optical computing and optical signal processing[35,36].

Here, we propose a miniaturized quantitative phase gradient microscope (QPGM) inspired by the classical DIC microscope and based on an integrated system of multifunctional dielectric metasurfaces. As we fully exploit the two unique properties of metasur-

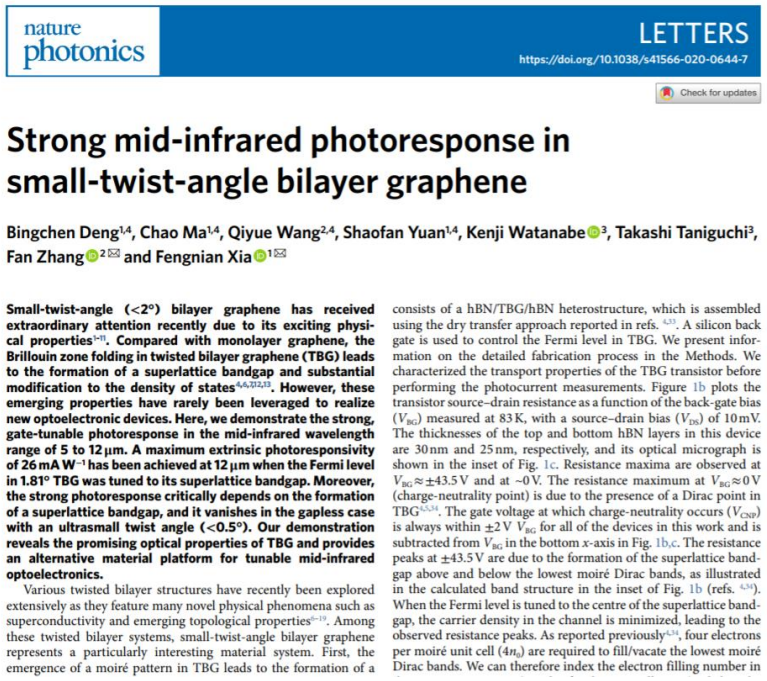

nature photonics
LETTERS
https://doi.org/10.1038/s41566-020-0644-7
Check for updates

Strong mid-infrared photoresponse in small-twist-angle bilayer graphene

Bingchen Deng[1,4], Chao Ma[1,4], Qiyue Wang[2,4], Shaofan Yuan[1,4], Kenji Watanabe[3], Takashi Taniguchi[3], Fan Zhang[2]✉ and Fengnian Xia[1]✉

Small-twist-angle (<2°) bilayer graphene has received extraordinary attention recently due to its exciting physical properties[1–11]. Compared with monolayer graphene, the Brillouin zone folding in twisted bilayer graphene (TBG) leads to the formation of a superlattice bandgap and substantial modification to the density of states[4,6,12,13]. However, these emerging properties have rarely been leveraged to realize new optoelectronic devices. Here, we demonstrate the strong, gate-tunable photoresponse in the mid-infrared wavelength range of 5 to 12 μm. A maximum extrinsic photoresponsivity of 26 mA W⁻¹ has been achieved at 12 μm when the Fermi level in 1.81° TBG was tuned to its superlattice bandgap. Moreover, the strong photoresponse critically depends on the formation of a superlattice bandgap, and it vanishes in the gapless case with an ultrasmall twist angle (<0.5°). Our demonstration reveals the promising optical properties of TBG and provides an alternative material platform for tunable mid-infrared optoelectronics.

Various twisted bilayer structures have recently been explored extensively as they feature many novel physical phenomena such as superconductivity and emerging topological properties[6–19]. Among these twisted bilayer systems, small-twist-angle bilayer graphene represents a particularly interesting material system. First, the emergence of a moiré pattern in TBG leads to the formation of a

consists of a hBN/TBG/hBN heterostructure, which is assembled using the dry transfer approach reported in refs. [4,33]. A silicon back gate is used to control the Fermi level in TBG. We present information on the detailed fabrication process in the Methods. We characterized the transport properties of the TBG transistor before performing the photocurrent measurements. Figure 1b plots the transistor source–drain resistance as a function of the back-gate bias (V_{BG}) measured at 83 K, with a source–drain bias (V_{DS}) of 10 mV. The thicknesses of the top and bottom hBN layers in this device are 30 nm and 25 nm, respectively, and its optical micrograph is shown in the inset of Fig. 1c. Resistance maxima are observed at $V_{BG} \approx \pm 43.5$ V and at ~0 V. The resistance maximum at $V_{BG} \approx 0$ V (charge-neutrality point) is due to the presence of a Dirac point in TBG[4,5,34]. The gate voltage at which charge-neutrality occurs (V_{CNP}) is always within ±2 V V_{BG} for all of the devices in this work and is subtracted from V_{BG} in the bottom x-axis in Fig. 1b,c. The resistance peaks at ±43.5 V are due to the formation of the superlattice bandgap above and below the lowest moiré Dirac bands, as illustrated in the calculated band structure in the inset of Fig. 1b (refs. [4,34]). When the Fermi level is tuned to the centre of the superlattice bandgap, the carrier density in the channel is minimized, leading to the observed resistance peaks. As reported previously[4,34], four electrons per moiré unit cell ($4n_0$) are required to fill/vacate the lowest moiré Dirac bands. We can therefore index the electron filling number in

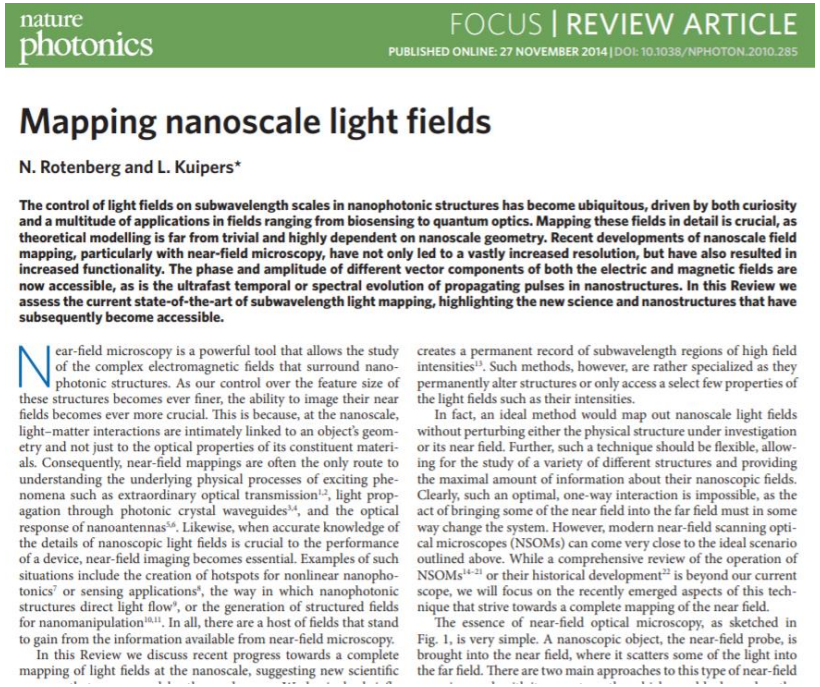

nature photonics
FOCUS | REVIEW ARTICLE
PUBLISHED ONLINE: 27 NOVEMBER 2014 | DOI: 10.1038/NPHOTON.2010.285

Mapping nanoscale light fields

N. Rotenberg and L. Kuipers*

The control of light fields on subwavelength scales in nanophotonic structures has become ubiquitous, driven by both curiosity and a multitude of applications in fields ranging from biosensing to quantum optics. Mapping these fields in detail is crucial, as theoretical modelling is far from trivial and highly dependent on nanoscale geometry. Recent developments of nanoscale field mapping, particularly with near-field microscopy, have not only led to a vastly increased resolution, but have also resulted in increased functionality. The phase and amplitude of different vector components of both the electric and magnetic fields are now accessible, as is the ultrafast temporal or spectral evolution of propagating pulses in nanostructures. In this Review we assess the current state-of-the-art of subwavelength light mapping, highlighting the new science and nanostructures that have subsequently become accessible.

Near-field microscopy is a powerful tool that allows the study of the complex electromagnetic fields that surround nanophotonic structures. As our control over the feature size of these structures becomes ever finer, the ability to image their near fields becomes ever more crucial. This is because, at the nanoscale, light–matter interactions are intimately linked to an object's geometry and not just to the optical properties of its constituent materials. Consequently, near-field mappings are often the only route to understanding the underlying physical processes of exciting phenomena such as extraordinary optical transmission[1,2], light propagation through photonic crystal waveguides[3,4], and the optical response of nanoantennas[5,6]. Likewise, when accurate knowledge of the details of nanoscopic light fields is crucial to the performance of a device, near-field imaging becomes essential. Examples of such situations include the creation of hotspots for nonlinear nanophotonics[7] or sensing applications[8], the way in which nanophotonic structures direct light flow[9], or the generation of structured fields for nanomanipulation[10,11]. In all, there are a host of fields that stand to gain from the information available from near-field microscopy.

In this Review we discuss recent progress towards a complete mapping of light fields at the nanoscale, suggesting new scientific

creates a permanent record of subwavelength regions of high field intensities[13]. Such methods, however, are rather specialized as they permanently alter structures or only access a select few properties of the light fields such as their intensities.

In fact, an ideal method would map out nanoscale light fields without perturbing either the physical structure under investigation or its near field. Further, such a technique should be flexible, allowing for the study of a variety of different structures and providing the maximal amount of information about their nanoscopic fields. Clearly, such an optimal, one-way interaction is impossible, as the act of bringing some of the near field into the far field must in some way change the system. However, modern near-field scanning optical microscopes (NSOMs) can come very close to the ideal scenario outlined above. While a comprehensive review of the operation of NSOMs[14–21] or their historical development[22] is beyond our current scope, we will focus on the recently emerged aspects of this technique that strive towards a complete mapping of the near field.

The essence of near-field optical microscopy, as sketched in Fig. 1, is very simple. A nanoscopic object, the near-field probe, is brought into the near field, where it scatters some of the light into the far field. There are two main approaches to this type of near-field

Druhy a struktura článku

- **Název**
- **Autoři (**+ afiliace**)**
- **Abstrakt** (= anotace)
- **Úvod** a vymezení problému
- **Dosažené výsledky a diskuze**
- **Závěr**
- Metody
- Poděkování a financování

ijmu

ntary information/matterials)

nature photonics

ARTICLES

https://doi.org/10.1038/s41566-019-0536-x

Single-shot quantitative phase gradient microscopy using a system of multifunctional metasurfaces

Hyounghan Kwon[1,2], Ehsan Arbabi[1,2], Seyedeh Mahsa Kamali[1,2], MohammadSadegh Faraji-Dana[1,2] and Andrei Faraon[1,2*]

Quantitative phase imaging (QPI) of transparent samples plays an essential role in multiple biomedical applications, and miniaturizing these systems will enable their adoption into point-of-care and in vivo applications. Here, we propose a compact quantitative phase gradient microscope (QGPM) based on two dielectric metasurface layers, inspired by a classical differential interference contrast (DIC) microscope. Owing to the multifunctionality and compactness of the dielectric metasurfaces, the QPGM simultaneously captures three DIC images to generate a quantitative phase gradient image in a single shot. The volume of the metasurface optical system is on the order of 1 mm³. Imaging experiments with various phase resolution samples verify the capability to capture quantitative phase gradient data, with phase gradient sensitivity better than 92.3 mrad μm⁻¹ and single-cell resolution. The results showcase the potential of metasurfaces for developing miniaturized QPI systems for label-free cellular imaging and point-of-care devices.

Optical phase microscopy techniques have been widely investigated for imaging transparent specimens like cells[1–4]. For these weakly scattering samples, phase information represents the optical path difference of light passing through the cell, which is usually directly related to its morphological and chemical properties[3]. Moreover, phase imaging techniques do not require contrast agents and avoid several issues faced in fluorescence microscopy such as photobleaching and phototoxicity[5]. Although conventional phase imaging methods such as phase contrast[1] and differential interference contrast (DIC) microscopy[2] only capture qualitative phase information, quantitative phase imaging (QPI) has been rapidly growing in the past two decades[3,4,6]. For

on-chip spectrometers[28,29] and endoscopes[30]. In addition, vertical integration of multiple metasurfaces has been introduced to achieve enhanced functionalities[31–34]. Despite these great advances, applications of metasurfaces for QPI have not previously been explored. Although different types of spatial field differentiator, which may be regarded as qualitative phase imaging devices, have been proposed, their investigation has been limited to optical computing and optical signal processing[35,36].

Here, we propose a miniaturized quantitative phase gradient microscope (QPGM) inspired by the classical DIC microscope and based on an integrated system of multifunctional dielectric metasurfaces. As we fully exploit the two unique properties of metasur-

Druhy a struktura článku

- **Název**
- **Autoři (**+afiliace**)**
- **Abstrakt** (Anotace)
- **Úvod** a vymezení problému
- **Dosažené výsledky a diskuze**
- **Závěr**
- Metody
- Poděkování a financování
- Autorské přínosy a (ne)konflikt zájmu
- **Reference**
- Doplňkové informace (Supplementary information/matterials)

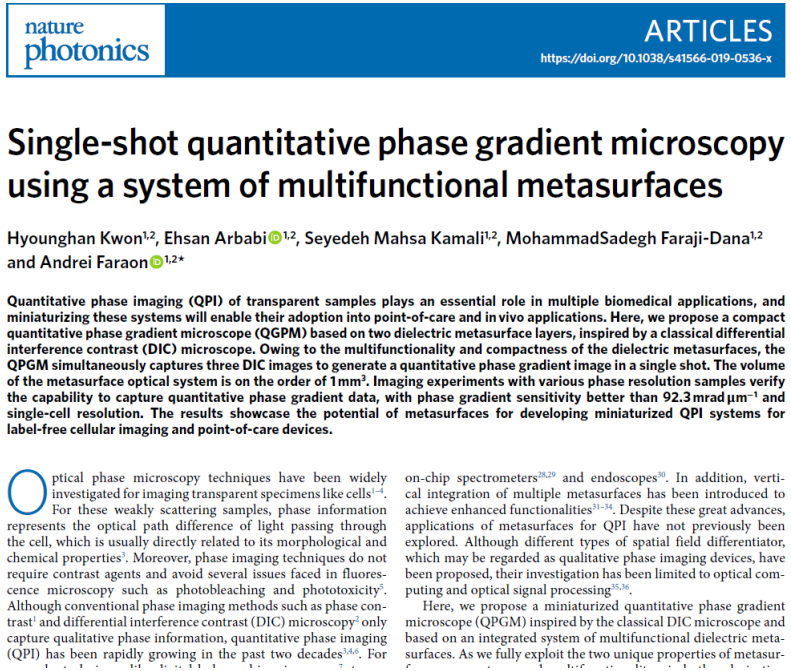

nature photonics

ARTICLES

https://doi.org/10.1038/s41566-019-0536-x

Single-shot quantitative phase gradient microscopy using a system of multifunctional metasurfaces

Hyounghan Kwon[1,2], Ehsan Arbabi[1,2], Seyedeh Mahsa Kamali[1,2], MohammadSadegh Faraji-Dana[1,2] and Andrei Faraon[1,2*]

Quantitative phase imaging (QPI) of transparent samples plays an essential role in multiple biomedical applications, and miniaturizing these systems will enable their adoption into point-of-care and in vivo applications. Here, we propose a compact quantitative phase gradient microscope (QGPM) based on two dielectric metasurface layers, inspired by a classical differential interference contrast (DIC) microscope. Owing to the multifunctionality and compactness of the dielectric metasurfaces, the QPGM simultaneously captures three DIC images to generate a quantitative phase gradient image in a single shot. The volume of the metasurface optical system is on the order of 1 mm³. Imaging experiments with various phase resolution samples verify the capability to capture quantitative phase gradient data, with phase gradient sensitivity better than 92.3 mrad μm⁻¹ and single-cell resolution. The results showcase the potential of metasurfaces for developing miniaturized QPI systems for label-free cellular imaging and point-of-care devices.

Optical phase microscopy techniques have been widely investigated for imaging transparent specimens like cells[1–4]. For these weakly scattering samples, phase information represents the optical path difference of light passing through the cell, which is usually directly related to its morphological and chemical properties[5]. Moreover, phase imaging techniques do not require contrast agents and avoid several issues faced in fluorescence microscopy such as photobleaching and phototoxicity[6]. Although conventional phase imaging methods such as phase contrast[1] and differential interference contrast (DIC) microscopy[2] only capture qualitative phase information, quantitative phase imaging (QPI) has been rapidly growing in the past two decades[3,4,6]. For

on-chip spectrometers[28,29] and endoscopes[30]. In addition, vertical integration of multiple metasurfaces has been introduced to achieve enhanced functionalities[31–34]. Despite these great advances, applications of metasurfaces for QPI have not previously been explored. Although different types of spatial field differentiator, which may be regarded as qualitative phase imaging devices, have been proposed, their investigation has been limited to optical computing and optical signal processing[35,36].

Here, we propose a miniaturized quantitative phase gradient microscope (QPGM) inspired by the classical DIC microscope and based on an integrated system of multifunctional dielectric metasurfaces. As we fully exploit the two unique properties of metasur-

Název => klíčová slova!

Single-shot quantitative phase gradient microscopy using a system of multifunctional metasurfaces

Druhy a struktura článku

- **Název**
- **Autoři (**+afiliace**)**
- **Abstrakt** (Anotace)
- **Úvod** a vymezení problému
- **Dosažené výsledky a diskuze**
- **Závěr**
- Metody
- Poděkování a financování
- Autorské přínosy a (ne)konflikt zájmu
- **Reference**
- Doplňkové informace (Supplementary information/matterials)

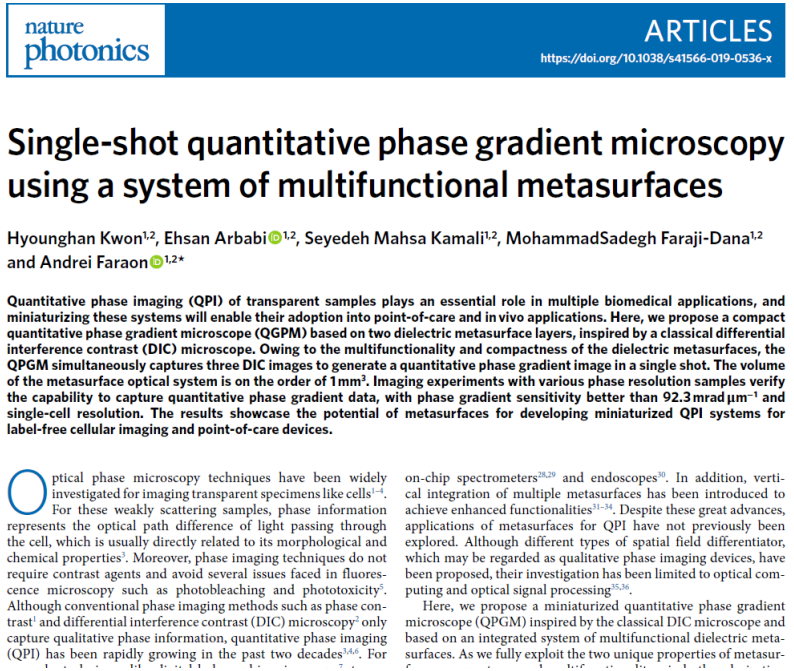

nature photonics ARTICLES
https://doi.org/10.1038/s41566-019-0536-x

Single-shot quantitative phase gradient microscopy using a system of multifunctional metasurfaces

Hyounghan Kwon[1,2], Ehsan Arbabi[1,2], Seyedeh Mahsa Kamali[1,2], MohammadSadegh Faraji-Dana[1,2] and Andrei Faraon[1,2*]

Quantitative phase imaging (QPI) of transparent samples plays an essential role in multiple biomedical applications, and miniaturizing these systems will enable their adoption into point-of-care and in vivo applications. Here, we propose a compact quantitative phase gradient microscope (QGPM) based on two dielectric metasurface layers, inspired by a classical differential interference contrast (DIC) microscope. Owing to the multifunctionality and compactness of the dielectric metasurfaces, the QPGM simultaneously captures three DIC images to generate a quantitative phase gradient image in a single shot. The volume of the metasurface optical system is on the order of 1 mm³. Imaging experiments with various phase resolution samples verify the capability to capture quantitative phase gradient data, with phase gradient sensitivity better than 92.3 mrad μm⁻¹ and single-cell resolution. The results showcase the potential of metasurfaces for developing miniaturized QPI systems for label-free cellular imaging and point-of-care devices.

Optical phase microscopy techniques have been widely investigated for imaging transparent specimens like cells[1–4]. For these weakly scattering samples, phase information represents the optical path difference of light passing through the cell, which is usually directly related to its morphological and chemical properties[5]. Moreover, phase imaging techniques do not require contrast agents and avoid several issues faced in fluorescence microscopy such as photobleaching and phototoxicity[6]. Although conventional phase imaging methods such as phase contrast[1] and differential interference contrast (DIC) microscopy[2] only capture qualitative phase information, quantitative phase imaging (QPI) has been rapidly growing in the past two decades[3,4,6]. For

on-chip spectrometers[28,29] and endoscopes[30]. In addition, vertical integration of multiple metasurfaces has been introduced to achieve enhanced functionalities[31–34]. Despite these great advances, applications of metasurfaces for QPI have not previously been explored. Although different types of spatial field differentiator, which may be regarded as qualitative phase imaging devices, have been proposed, their investigation has been limited to optical computing and optical signal processing[35,36].

Here, we propose a miniaturized quantitative phase gradient microscope (QPGM) inspired by the classical DIC microscope and based on an integrated system of multifunctional dielectric metasurfaces. As we fully exploit the two unique properties of metasur-

Autoři a afiliace

Hyounghan Kwon[1,2], Ehsan Arbabi[1,2], Seyedeh Mahsa Kamali[1,2], MohammadSadegh Faraji-Dana[1,2] and Andrei Faraon[1,2*]

[1]T. J. Watson Laboratory of Applied Physics and Kavli Nanoscience Institute, California Institute of Technology, Pasadena, CA, USA. [2]Department of Electrical Engineering, California Institute of Technology, Pasadena, CA, USA. *e-mail: faraon@caltech.edu

ORCID

https://orcid.org/0000-0003-0346-4110

Druhy a struktura článku

- **Název**
- **Autoři (**+afiliace**)**
- **Abstrakt** (Anotace)
- **Úvod** a vymezení problému
- **Dosažené výsledky a diskuze**
- **Závěr**
- Metody
- Poděkování a financování
- Autorské přínosy a (ne)konflikt zájmu
- **Reference**
- Doplňkové informace (Supplementary information/matterials)

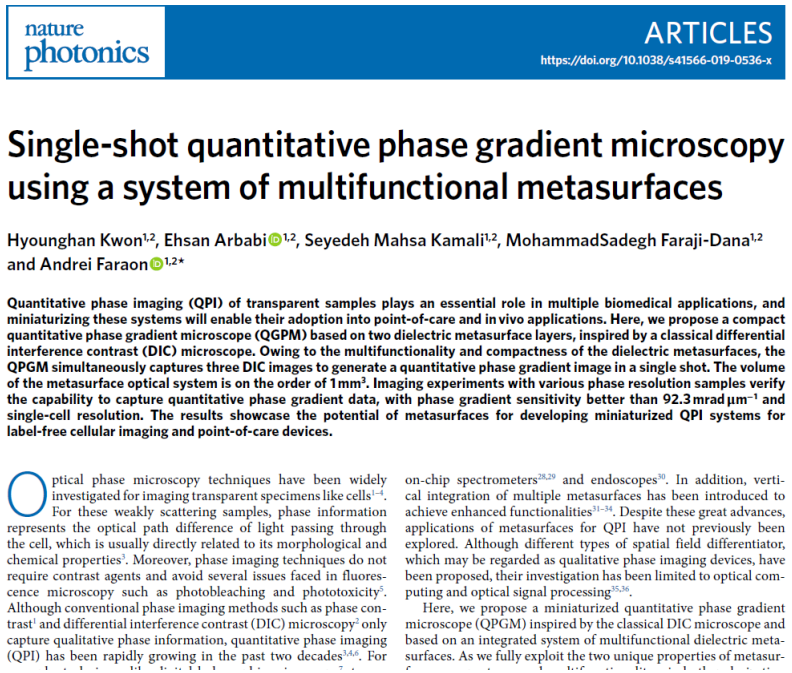

nature photonics ARTICLES
https://doi.org/10.1038/s41566-019-0536-x

Single-shot quantitative phase gradient microscopy using a system of multifunctional metasurfaces

Hyounghan Kwon[1,2], Ehsan Arbabi[1,2], Seyedeh Mahsa Kamali[1,2], MohammadSadegh Faraji-Dana[1,2] and Andrei Faraon[1,2*]

Quantitative phase imaging (QPI) of transparent samples plays an essential role in multiple biomedical applications, and miniaturizing these systems will enable their adoption into point-of-care and in vivo applications. Here, we propose a compact quantitative phase gradient microscope (QGPM) based on two dielectric metasurface layers, inspired by a classical differential interference contrast (DIC) microscope. Owing to the multifunctionality and compactness of the dielectric metasurfaces, the QPGM simultaneously captures three DIC images to generate a quantitative phase gradient image in a single shot. The volume of the metasurface optical system is on the order of 1 mm³. Imaging experiments with various phase resolution samples verify the capability to capture quantitative phase gradient data, with phase gradient sensitivity better than 92.3 mrad μm⁻¹ and single-cell resolution. The results showcase the potential of metasurfaces for developing miniaturized QPI systems for label-free cellular imaging and point-of-care devices.

Optical phase microscopy techniques have been widely investigated for imaging transparent specimens like cells[1–4]. For these weakly scattering samples, phase information represents the optical path difference of light passing through the cell, which is usually directly related to its morphological and chemical properties[5]. Moreover, phase imaging techniques do not require contrast agents and avoid several issues faced in fluorescence microscopy such as photobleaching and phototoxicity[6]. Although conventional phase imaging methods such as phase contrast[1] and differential interference contrast (DIC) microscopy[2] only capture qualitative phase information, quantitative phase imaging (QPI) has been rapidly growing in the past two decades[3,4,6]. For

on-chip spectrometers[28,29] and endoscopes[30]. In addition, vertical integration of multiple metasurfaces has been introduced to achieve enhanced functionalities[31–34]. Despite these great advances, applications of metasurfaces for QPI have not previously been explored. Although different types of spatial field differentiator, which may be regarded as qualitative phase imaging devices, have been proposed, their investigation has been limited to optical computing and optical signal processing[35,36].

Here, we propose a miniaturized quantitative phase gradient microscope (QPGM) inspired by the classical DIC microscope and based on an integrated system of multifunctional dielectric metasurfaces. As we fully exploit the two unique properties of metasur-

Abstrakt => lákadlo!

Quantitative phase imaging (QPI) of transparent samples plays an essential role in multiple biomedical applications, and miniaturizing these systems will enable their adoption into point-of-care and in vivo applications. Here, we propose a compact quantitative phase gradient microscope (QGPM) based on two dielectric metasurface layers, inspired by a classical differential interference contrast (DIC) microscope. Owing to the multifunctionality and compactness of the dielectric metasurfaces, the QPGM simultaneously captures three DIC images to generate a quantitative phase gradient image in a single shot. The volume of the metasurface optical system is on the order of 1 mm³. Imaging experiments with various phase resolution samples verify the capability to capture quantitative phase gradient data, with phase gradient sensitivity better than 92.3 mrad μm⁻¹ and single-cell resolution. The results showcase the potential of metasurfaces for developing miniaturized QPI systems for label-free cellular imaging and point-of-care devices.

Úvod (Introduction)

soubory citací a většina citací článku

Podobné a přelomové citace (dle klíčových slov)
vs.
vymezení se vůči nim (v čem jste unikátní)

Optical phase microscopy techniques have been widely investigated for imaging transparent specimens like cells[1–4]. For these weakly scattering samples, phase information represents the optical path difference of light passing through the cell, which is usually directly related to its morphological and chemical properties[3]. Moreover, phase imaging techniques do not require contrast agents and avoid several issues faced in fluorescence microscopy such as photobleaching and phototoxicity[5]. Although conventional phase imaging methods such as phase contrast[1] and differential interference contrast (DIC) microscopy[2] only capture qualitative phase information, quantitative phase imaging (QPI) has been rapidly growing in the past two decades[3,4,6]. For example, techniques like digital holographic microscopy[7], tomographic QPI[8,9], Fourier ptychography[10] and lensless imaging[11] overcome limitations of qualitative phase imaging methods to acquire quantitative phase data.

Miniaturized microscopes have garnered great interest in recent decades[12–14] because they enable and facilitate in vivo biological imaging in freely moving objects[14] and in portable applications. Miniaturized systems have only been demonstrated as different forms of amplitude imaging modules such as single-photon[12] or two-photon[13] fluorescence microscopes. This is mainly because QPI systems usually require an interference 'set-up' to retrieve the phase information, and such set-ups need complicated and bulky optical systems. This left the miniaturized QPI microscopes that are of interest in various fields such as biomedicine[4] out of reach until now.

Dielectric metasurfaces are a category of diffractive optical elements consisting of nanoscatterers[15,16] that enable the control of light in subwavelength scales[17–22]. In addition, metasurfaces can simultaneously provide multiple distinct functionalities through various schemes such as spatial multiplexing[23,24] or more sophisticated designs of the nanoscatterers[25,26]. These capabilities, compactness, low weight and compatibility with conventional nanofabrication processes have made them suitable candidates for miniaturized optical devices such as miniaturized microscopes[27], on-chip spectrometers[28,29] and endoscopes[30]. In addition, vertical integration of multiple metasurfaces has been introduced to achieve enhanced functionalities[31–34]. Despite these great advances, applications of metasurfaces for QPI have not previously been explored. Although different types of spatial field differentiator, which may be regarded as qualitative phase imaging devices, have been proposed, their investigation has been limited to optical computing and optical signal processing[35,36].

Here, we propose a miniaturized quantitative phase gradient microscope (QPGM) inspired by the classical DIC microscope and based on an integrated system of multifunctional dielectric metasurfaces. As we fully exploit the two unique properties of metasurfaces, compactness and multifunctionality, via both polarization and spatial multiplexing methods, two metasurface layers that are cascaded vertically operate as a miniaturized QPGM. We experimentally demonstrate that the millimetre-scale optical device can capture quantitative phase gradient images (PGIs) from phase resolution targets and biological samples.

„malý" abstrakt toho, co se odborně udělalo

Results

Concept of the metasurface-based QPGM. Figure 1a illustrates the concept of a miniaturized QPGM consisting of two cascaded metasurface layers. The roles of each layer are explained visually in Fig. 1b. Metasurface layer 1 captures two images for transverse electric (TE) and transverse magnetic (TM) polarizations with focal points that are separated along the *y* axis. In addition, it splits the captured light equally into three separate directions towards the three metasurface lenses in layer 2. To implement this multifunctionality, polarization[20] and spatial multiplexing techniques[23,24] are employed in the design of metasurface layer 1 (see Supplementary Note 1 for details). Metasurface layer 2, which is composed of three birefringent off-axis lenses, forms three DIC images with three different phase offsets between the TE and TM polarizations. Effectively, each metasurface of the second layer constitutes a separate DIC microscope system with the metasurface layer 1. With two linear polarizers at the input and output aligned to 45° and −45°,

Výsledky (Results)

3-4 bloky obrázků a jejich popis/vysvětlení
<=>
je nutné mít „dobré“ výsledky
Nesmí být logické skoky
<=>
návaznost vět a odstavců
případně citace nebo podpůrné materiály

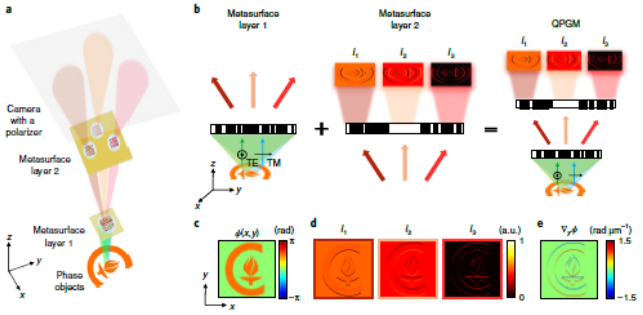

Fig. 1 | Schematic of a metasurface-based QPGM and its operation principle. a, Schematic of the QPGM employing two metasurface layers, where the second layer is composed of three separate metasurface lenses. The first metasurface, together with each of the lenses in the second metasurface layer, forms a different image of the object. A polarizer and the polarization-sensitive metasurfaces then result in three interference patterns. **b**, Illustration of the roles of the two metasurface layers. Metasurface 1 makes two sheared focuses for TE and TM polarizations and splits the field in three different directions towards the three lenses in the second layer. With the polarizer, the three metasurface lenses in layer 2 form three DIC images (I_1, I_2 and I_3) having different phase offsets between the TE and TM polarizations. The combination of the two layers forms the QPGM shown on the right. **c**, A binary phase sample with unity amplitude used as an example target. **d**, Set of three DIC images of the phase sample shown in **c**. **e**, PGI formed from combining I_1, I_2 and I_3 from **d**, showing the phase gradient along the *y* axis. The *y* axis lies along the shear direction of the system.

respectively, the two metasurface layers capture three separate DIC images with different phase offsets. As an example, a binary phase target is shown in Fig. 1c, which has optical fields with unity amplitude, $U(x, y) = e^{i\phi(x,y)}$. The QPGM simultaneously captures three DIC images (I_1, I_2 and I_3), as shown in Fig. 1d. Specifically, I_1, I_2 and I_3 are written as

$$I_j = |U(x,y) - e^{i\phi_j} U(x, y - \Delta y)| \quad (1)$$

where $\phi_j = \phi_0 + \frac{2\pi}{3}(j-1)$ and Δy is the sheared distance between TE and TM polarizations at the object plane. I_1, I_2 and I_3 in Fig. 1d show a strong contrast at the top and bottom edges of the sample because each DIC image results from the interference of the two sheared optical fields along the *y* axis by equation (1). Using I_1, I_2 and I_3, one can calculate the unidirectional gradient of the phase sample with respect to *y*, $\nabla_y\phi(x, y)$, through the three-step phase shifting method[37]:

$$\nabla_y\phi = \frac{1}{\Delta y}\arctan\left(\sqrt{3}\frac{I_2 - I_3}{2I_1 - I_2 - I_3}\right) - \nabla_y\phi_{cal} \quad (2)$$

Here, $\nabla_y\phi_{cal}$ is the PGI calculated in the absence of the sample that is used for calibration (see Supplementary Note 3 for details about the three-step phase shifting method). Figure 1e shows the PGI calculated from the three DIC images in Fig. 1d.

The QPGM consists of the two multifunctional metasurface layers for two main reasons (see Supplementary Note 1 and Supplementary Fig. 1 for detailed discussion based on wave propagation simulations). First, at least two polarization-sensitive bifocal lenses are needed to capture clear DIC images. In other words, a single birefringent metasurface lens with a regular refractive lens is not capable of capturing the DIC images clearly (see Supplementary Note 2 and Supplementary Fig. 2 for theoretical and experimental results with the single metasurface lens). Second, the vertical integration of the two multifunctional metasurface layers uniquely enables capturing the PGI in a single shot with compact implementation of the system.

We should mention that while single polarization-sensitive bifocal metasurface lenses have been demonstrated before for polarization splitting and imaging[20,38], their potential application for phase imaging has not been explored. Moreover, the working principle used here is conceptually similar to gradient light interference microscopy, as in both methods several DIC images are utilized to calculate the quantitative phase gradient image along one axis[39]. Various devices also have been proposed to develop compact QPI techniques[40–44]. However, they are designed as add-on devices to a conventional microscope system and their imaging performances mainly rely on the microscope, which is fundamentally hard to miniaturize. The system demonstrated here differs from previous approaches in that the highly miniaturized system replaces the bulky phase or phase gradient microscope systems and captures the phase gradient information in a single shot without additional phase shifting elements like variable liquid-crystal retarders or spatial light modulators.

In the following we discuss two implementations of the QPGM, one based on metasurfaces on two separate substrates and one composed of metasurfaces on both sides of a single substrate. Although the first implementation provides large aperture size and field of view, the second implementation provides compactness and mechanical robustness.

Implementation of the QPGM by two separate dielectric metasurface layers. To implement the two metasurface layers, we utilized a high-contrast transmitarray platform consisting of rectangular amorphous silicon nanoposts on a fused-silica substrate, as shown in Fig. 2a (see Methods and Supplementary Fig. 4 for details)[20]. We designed the metasurfaces for an operation wavelength of 850 nm. In Fig. 2b,c, schematics of the metasurface-based QPGM

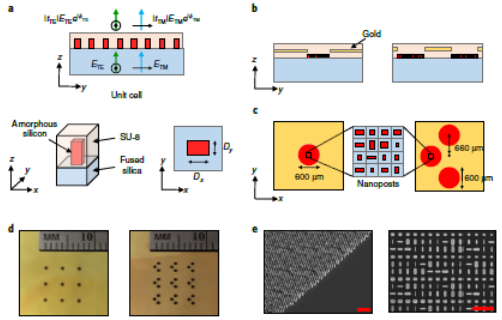

Fig. 2 | Design and fabrication of the metasurfaces. a, Schematics of a uniform array of rectangular nanoposts (top) and a single unit cell (bottom), showing the parameter definitions. The rectangular amorphous silicon nanoposts are located on a fused-silica substrate, cladded by an 8-μm-thick SU-8 layer for protection. The transmission phase of the two orthogonal polarizations can be independently controlled using the nanoposts. The amorphous silicon layer is 664 nm thick, and the lattice constant is 380 nm. **b**, Schematic side views of metasurface layers 1 (left) and 2 (right), showing the gold apertures used to block unwanted diffraction and the external noise. **c**, Schematic top views of metasurface layers 1 (left) and 2 (right). A magnified view of the array of nanoposts is shown at the centre. **d**, Optical images of the fabricated metasurfaces. Nine copies of the fabricated metasurface-based QPGM system are shown. **e**, SEM images of a portion of the fabricated metasurfaces. Scale bars, 2 μm (left) and 1 μm (right).

are presented. The left and right images correspond to metasurface layers 1 and 2 in Fig. 1a,b, respectively. To minimize the effects of geometric aberrations, the phase profiles of the metasurfaces were further optimized using the ray-tracing method (Zemax OpticStudio) over a field of view (FOV) with diameter of 140 μm (see Methods, Supplementary Note 1, Supplementary Table 1 and Supplementary Fig. 5 for details of the optimized phase profiles and corresponding point spread functions).

Conventional nanofabrication techniques were used to fabricate the metasurfaces (see Methods for the process details). All four metasurface lenses have identical diameters of 600 μm. To block the stray light caused by imperfect operation of the metasurfaces and limit the device aperture, circular gold apertures were patterned using photolithography. Figure 2d,e presents optical and scanning electron microscope (SEM) images of the two layers of the fabricated metasurfaces. In this design, the whole QPGM system would fit within a cube measuring 1.92 × 1.26 × 2.70 mm³, including the space between the metasurfaces. The magnification and objective numerical aperture (NA) of the QPGM are ×1.98 and 0.4, respectively. Although the phase map is optimized for the central area (140 μm diameter), the total FOV of the system is 336 μm in diameter. In addition, the separation between the optical axes for TE and TM polarizations is 1.5 μm, which results in a derivation step of $\Delta y = 2.25$ μm (see Supplementary Fig. 3 for details about Δy). Δy is larger than 1.06 μm, the theoretical diffraction limit of the imaging system, and it imposes a constraint on the resolution along the *y* axis. However, we should point out that Δy can easily be adjusted to below the diffraction-limited resolution by reducing the optical axis separation accordingly.

Imaging with the QPGM based on two separate metasurface layers. We characterized the QPGM, consisting of the fabricated metasurfaces, with a commercially available 1951 USAF phase resolution target (Quantitative Phase Microscopy Target, Benchmark Technologies). As shown in Fig. 3a, the QPGM captured three DIC images of the 314-nm-thick resolution target in a single shot (see Methods and Supplementary Fig. 6 for details of the optical set-up). The resulting PGI, shown in Fig. 3b, is calculated from the DIC images in Fig. 3a using equation (2). As expected in the ideal cases in Fig. 1d,e, the unidirectional phase gradient imaging in the *y* direction causes a strong contrast only at the top and bottom edges, and very weak contrast at the left and right edges. This is also seen in the measurement results shown in Fig. 3a,b. To verify the QPGM capability, we used seven parts of the resolution target with thicknesses ranging from 54 to 371 nm. Figure 3c shows the resulting PGIs for 105-nm-, 207-nm- and 314-nm-thick resolution targets (see Supplementary Fig. 7 for the four remaining PGIs). The results show a clear increase in the phase gradient as the thickness of the structures increases. For a more rigorous analysis, Fig. 3d shows the target thicknesses estimated from the PGIs, in addition to the values measured using atomic force microscopy (AFM). The agreement between these measurements shows the ability of the system to retrieve quantitative phase data. To estimate the target thickness, the phase gradient is integrated at the edges of the targets along the *y* axis to calculate the phase. The thickness is then estimated from the phase, the refractive index of the polymer constituting the target and the wavelength. The QPGM can clearly capture phase gradient information as small as 92.3 mrad μm^{-1}, which corresponds to a phase of 207 mrad (see Supplementary Fig. 7a for details). In addition, the measured spatial and temporal noise levels are 36.9 ± 0.7 and 11.4 mrad μm^{-1}, respectively (see Supplementary Fig. 8 for details). Furthermore, the lateral resolutions achieved in the experiment along the *x* and *y* axes are 2.76 μm and 3.48 μm, respectively (see Supplementary Fig. 9 for details). Compared with the 1.06 μm theoretical diffraction limit, the reduced resolutions result from the geometric aberration of the device, misalignment in

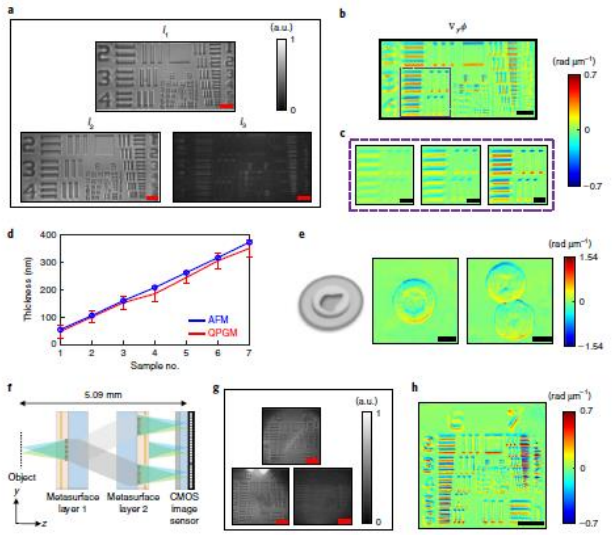

Fig. 3 | Imaging experiment with the QPGM based on two separate metasurface layers. a, Three DIC images of a 314-nm-thick QPI 1951-USAF resolution target captured by the QPGM. Scale bars, 25 μm. **b**, The PGI calculated from the DIC images in **a**. Scale bar, 25 μm. **c**, The PGIs captured for three parts of the phase targets with thicknesses of 105 nm, 207 nm and 314 nm (left to right), respectively. Scale bars, 15 μm. **d**, Thicknesses of seven different phase targets calculated by the QPGM, and those measured by AFM. The plotted thicknesses estimated with the QPGM are averaged over 100 arbitrarily chosen points on the sample edges. Error bars represent standard deviations of the estimated values. **e**, Schematic of a sea urchin cell and its corresponding PGIs. Scale bars, 40 μm. **f**, Schematic of the miniaturized optical set-up. The microscope consists of the two metasurfaces shown in Fig. 2d, a CMOS image sensor and a linear polarizer attached to the sensor. **g**, Three DIC images captured by the set-up in **f**. The 314-nm-thick resolution target used in **a** is imaged. Scale bars, 50 μm. **h**, The PGI calculated from the DIC images in **g**. Scale bar, 50 μm.

the optical set-up and imperfect fabrication. To compare our results with one of the state-of-the-art QPI techniques, the resolution targets were also characterized by Fourier ptychography techniques[10] (see Supplementary Fig. 10 for details). Finally, to demonstrate the capability of the QPGM to image biological samples, we imaged several sea urchin samples. As seen in a few sample PGIs, plotted in Fig. 3e, the QPGM can capture the edges of the sea urchin as well as the detailed morphology inside the cells. Thus, the QPGM is able to measure the phase gradient information of the biological samples, which is directly related to cellular mass transport[39].

To demonstrate further miniaturization of the system, we performed additional measurements with an off-the-shelf CMOS image sensor. Figure 3f presents a schematic of the optical system. The distance from the object plane to the CMOS image sensor is just 5.09 mm (see Supplementary Fig. 11a,b for details of the compact optical set-up). Figure 3g shows three raw DIC images captured by the set-up in Fig. 3f when using the imaging target shown in Fig. 3a. Using equation (2), the three DIC images in Fig. 3g result in the PGI plotted in Fig. 3h. The edges and the measured phase gradient of the PGI in Fig. 3h are comparable to the results shown in Fig. 3b (see Supplementary Fig. 11c,d for additional measurement results).

QPGM based on monolithically integrated double-sided metasurfaces. To further miniaturize the device, we designed and fabricated a monolithically integrated double-sided metasurface QPGM. Figure 4a schematically illustrates the double-sided QPGM. Although conceptually similar to the system discussed in the previous section, the double-sided QPGM is more compact, mechanically robust and does not need further alignment after fabrication. The two metasurface layers are based on the same platform discussed in the previous section, but they are fabricated on the two sides of a 1-mm-thick fused-silica substrate (see Methods, Supplementary Note 1 and Supplementary Table 2 for details about the design and fabrication). The optical images of the device are shown in Fig. 4b. The total volume of the QPGM is 0.62 × 0.41 × 1.00 mm³, it has a magnification of ×1.60 and a FOV with diameter of 140 μm. To verify the capability of the double-sided QPGM, we used the same resolution targets as in Fig. 3c,d. The results, shown in Fig. 4c,d,

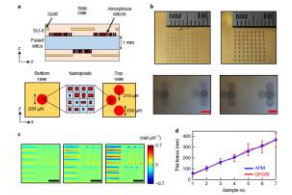

Nikdy nepodvádět! Čtenář je chytrý!

Výsledky (Results) - obrázky

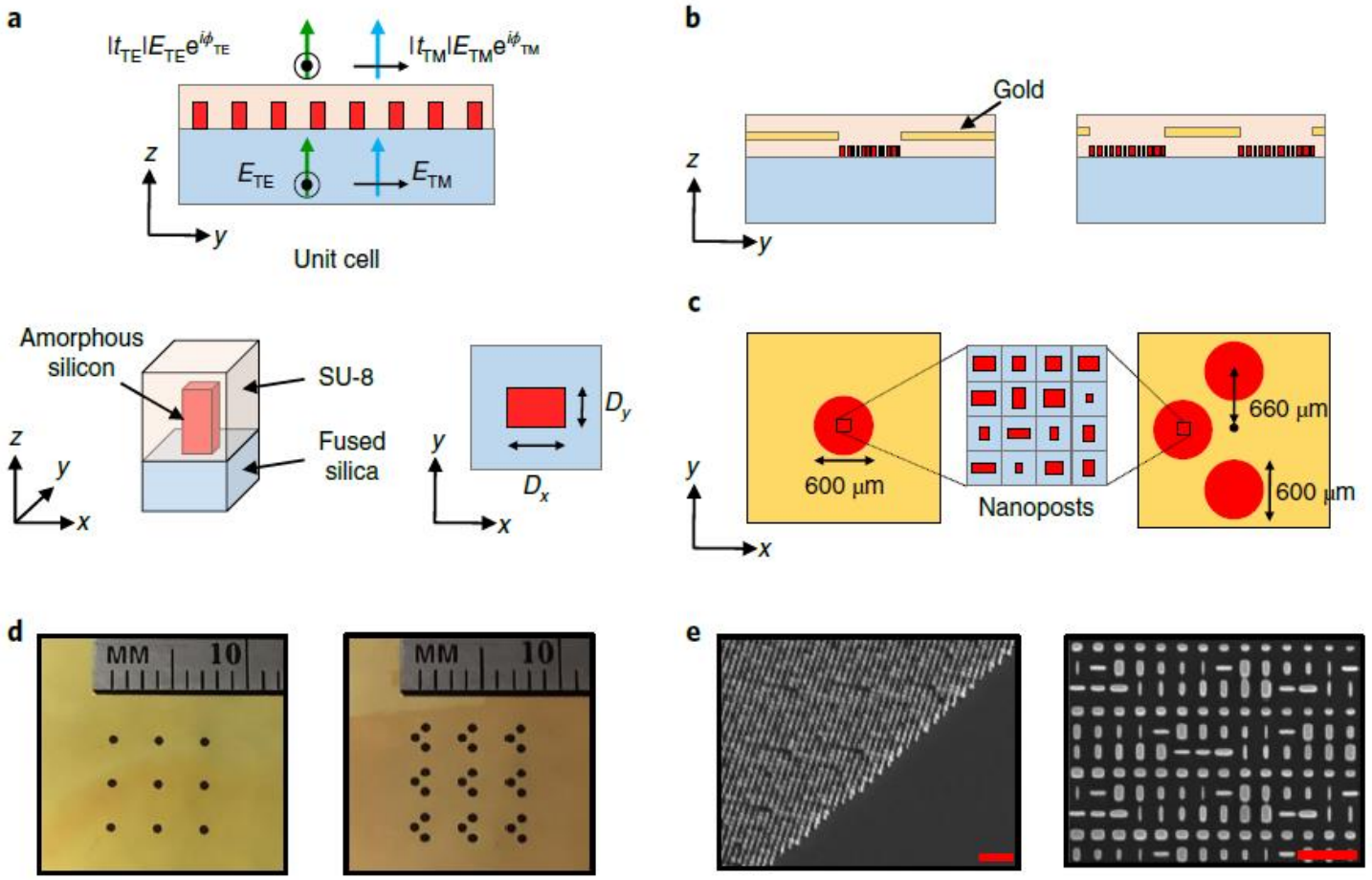

Fig. 2 | Design and fabrication of the metasurfaces. a, Schematics of a uniform array of rectangular nanoposts (top) and a single unit cell (bottom), showing the parameter definitions. The rectangular amorphous silicon nanoposts are located on a fused-silica substrate, cladded by an 8-μm-thick SU-8 layer for protection. The transmission phase of the two orthogonal polarizations can be independently controlled using the nanoposts. The amorphous silicon layer is 664 nm thick, and the lattice constant is 380 nm. **b**, Schematic side views of metasurface layers 1 (left) and 2 (right), showing the gold apertures used to block unwanted diffraction and the external noise. **c**, Schematic top views of metasurface layers 1 (left) and 2 (right). A magnified view of the array of nanoposts is shown at the centre. **d**, Optical images of the fabricated metasurfaces. Nine copies of the fabricated metasurface-based QPGM system are shown. **e**, SEM images of a portion of the fabricated metasurfaces. Scale bars, 2 μm (left) and 1 μm (right).

Výsledky

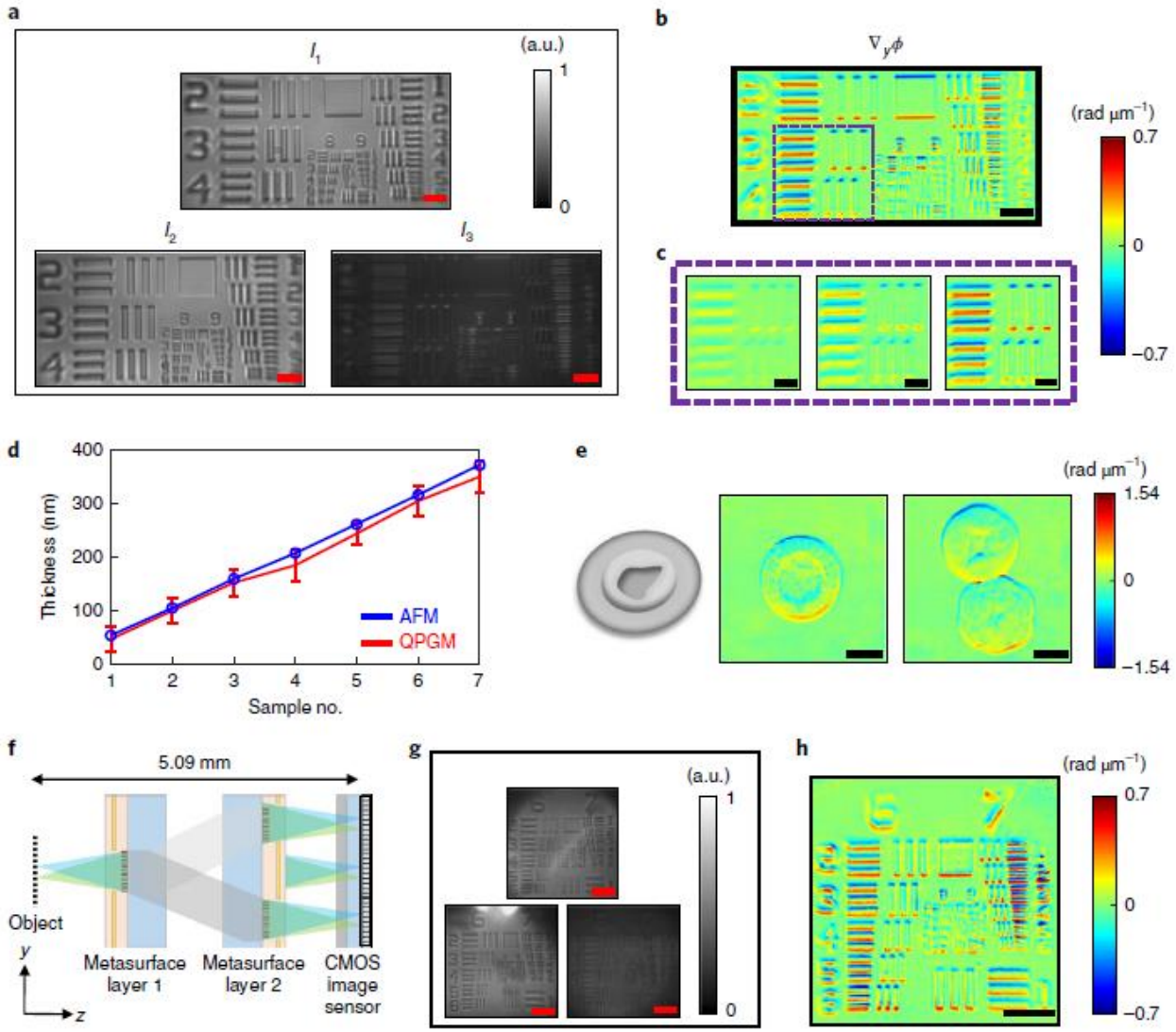

Fig. 3 | Imaging experiment with the QPGM based on two separate metasurface layers. a, Three DIC images of a 314-nm-thick QPI 1951-USAF resolution target captured by the QPGM. Scale bars, 25 μm. **b**, The PGI calculated from the DIC images in **a**. Scale bar, 25 μm. **c**, The PGIs captured for three parts of the phase targets with thicknesses of 105 nm, 207 nm and 314 nm (left to right), respectively. Scale bars, 15 μm. **d**, Thicknesses of seven different phase targets calculated by the QPGM, and those measured by AFM. The plotted thicknesses estimated with the QPGM are averaged over 100 arbitrarily chosen points on the sample edges. Error bars represent standard deviations of the estimated values. **e**, Schematic of a sea urchin cell and its corresponding PGIs. Scale bars, 40 μm. **f**, Schematic of the miniaturized optical set-up. The microscope consists of the two metasurfaces shown in Fig. 2d, a CMOS image sensor and a linear polarizer attached to the sensor. **g**, Three DIC images captured by the set-up in **f**. The 314-nm-thick resolution target used in **a** is imaged. Scale bars, 50 μm. **h**, The PGI calculated from the DIC images in **g**. Scale bar, 50 μm.

Diskuze (Discussion)

Slabiny výsledků a jejich příčiny případně hypotetické návrhy na vylepšení (plán do budoucnosti)

verify that the double-sided metasurface QPGM generates PGIs that are comparable to those of the QPGM based on the two separate metasurface layers. In particular, the estimated thicknesses of the phase samples plotted in Fig. 4d are in good agreement with the values measured by AFM. Phase images of sea urchin samples, captured by the double-sided metasurface QPGM, are shown in Supplementary Fig. 12.

Discussion

One limitation of the proposed system, especially for the double-sided metasurface device, is its FOV. The small FOV mostly results from the fact that our system is close to a $4-f$ configuration that requires the sum of the focal lengths of the two lenses to be comparable to their separation. To increase the FOV, a possible solution is the recently reported folded metasurface platform[29], which might be able to achieve a large FOV and a small footprint simultaneously. In this platform, the propagation space between the two lenses is folded inside the substrate through multiple reflections, and therefore the effective distance between the lenses can be significantly larger than the substrate thickness. Furthermore, adding another metasurface layer can be used to mitigate the geometric aberrations further and increase the FOV[31].

The QPGM system is sensitive to the equality of optical axis separation for TE and TM polarizations in the two metasurface lenses. Nevertheless, this separation can be controlled very precisely because metasurfaces allow for implementation of almost arbitrary phase profiles in subwavelength scales. If the separations between the optical axes are identical for the two metasurfaces, the structure becomes robust against lateral and axial misalignment (Supplementary Fig. 13).

Outlook and summary

It is worth noting that the multifunctionality via both polarization and spatial multiplexing schemes, which is the key property for the design of the miniaturized QPGM, is very hard to achieve in any other platform, if at all. We envision that these and other versatile properties of metasurfaces enable various types of quantitative phase imaging devices. For example, three different images at different axial positions can be captured to calculate the phase information rather than the phase gradient information through the transport-of-intensity equation[11,45]. In addition, different focus scanning schemes can be integrated with the QPGM to achieve a tomographic quantitative phase imaging device with fast axial scanning[46–48]. Moreover, we expect that around ten to a hundred of the miniaturized microscopes could be integrated on a single CMOS sensor for highly parallelized microscopy. Finally, a synergistic combination of the metasurfaces and computational optics is an emerging area for enhancing the potentials of metasurface optical systems. Considering the computational aspects of quantitative phase imaging, we believe that new kinds of miniaturized quantitative phase imaging device that will benefit from the enhanced optical control of the metasurfaces can be proposed.

In conclusion, we utilized two multifunctional metasurface layers to realize miniaturized quantitative phase gradient microscopes. The design and working principle were proposed and investigated both through simulation and experiment. Utilizing vertically integrated multifunctional metasurfaces, we experimentally captured phase gradient images of several transparent samples and verified the quantitative phase imaging capability of the systems. This work clearly demonstrates potentials of dielectric metasurface platforms in quantitative phase imaging systems to make miniaturized imaging

Závěr (Conclusion)

Klidně diskutujte!

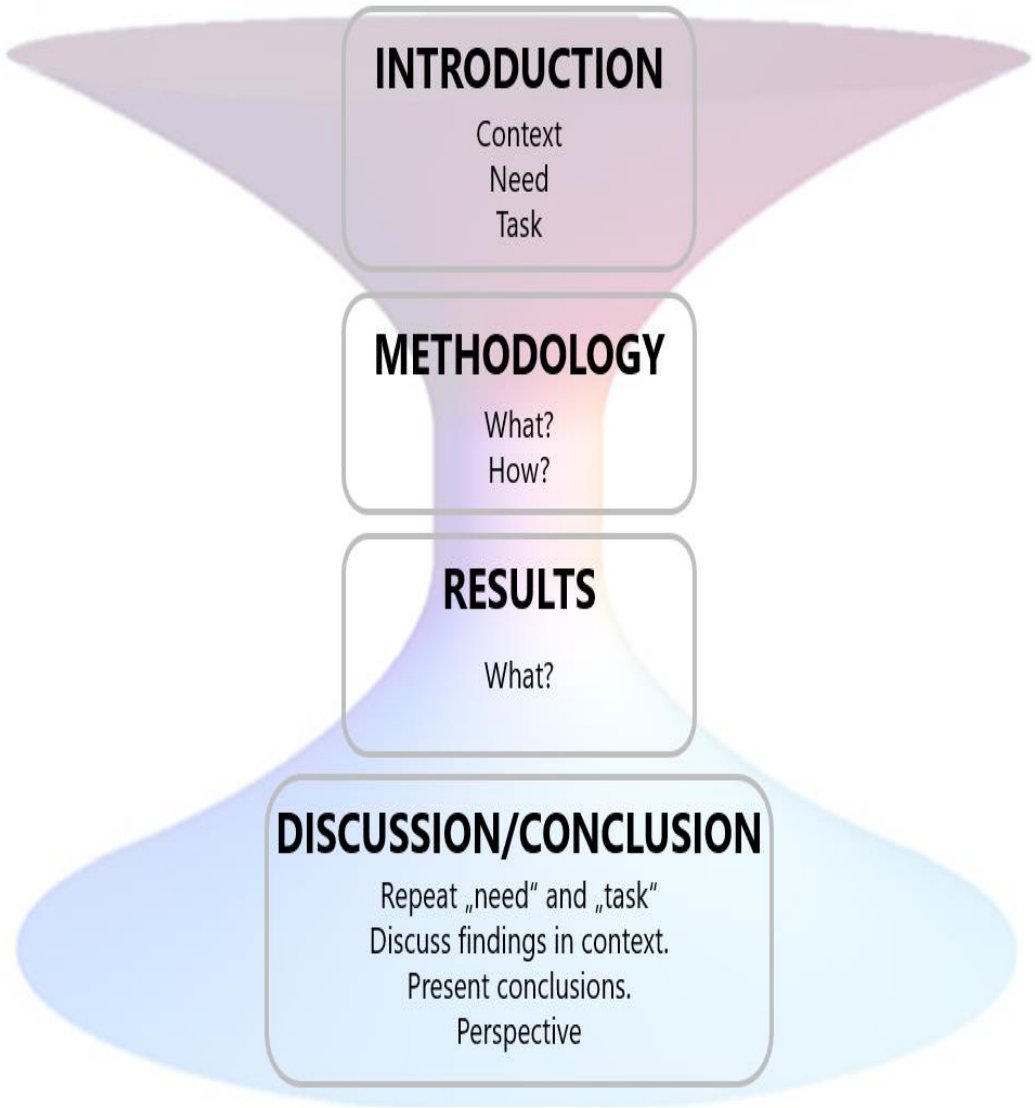

„Wormhole scheme"

Váš závěr (velmi důležitý! Vyvrcholení článku)
Silné a „sexy" věty + konkrétní aplikace

Obecný závěr a příprava/stupňování na váš závěr
(přesah článku, unikátnost, vysoký impakt na vědu)

Outlook and summary

It is worth noting that the multifunctionality via both polarization and spatial multiplexing schemes, which is the key property for the design of the miniaturized QPGM, is very hard to achieve in any other platform, if at all. We envision that these and other versatile properties of metasurfaces enable various types of quantitative phase imaging devices. For example, three different images at different axial positions can be captured to calculate the phase information rather than the phase gradient information through the transport-of-intensity equation[11,45]. In addition, different focus scanning schemes can be integrated with the QPGM to achieve a tomographic quantitative phase imaging device with fast axial scanning[46–48]. Moreover, we expect that around ten to a hundred of the miniaturized microscopes could be integrated on a single CMOS sensor for highly parallelized microscopy. Finally, a synergistic combination of the metasurfaces and computational optics is an emerging area for enhancing the potentials of metasurface optical systems. Considering the computational aspects of quantitative phase imaging, we believe that new kinds of miniaturized quantitative phase imaging device that will benefit from the enhanced optical control of the metasurfaces can be proposed.

In conclusion, we utilized two multifunctional metasurface layers to realize miniaturized quantitative phase gradient microscopes. The design and working principle were proposed and investigated both through simulation and experiment. Utilizing vertically integrated multifunctional metasurfaces, we experimentally captured phase gradient images of several transparent samples and verified the quantitative phase imaging capability of the systems. This work clearly demonstrates potentials of dielectric metasurface platforms in quantitative phase imaging systems to make miniaturized imaging devices such as miniaturized microscopes or endoscopes[30]. With the current great interest in quantitative phase imaging and miniaturized microscopes, we envision that the metasurfaces will play a significant role in the development of these technologies.

Odkaz na on-line verzi (DOI článku)

Reference/citace

devices such as miniaturized microscopes or endoscopes[30]. With the current great interest in quantitative phase imaging and miniaturized microscopes, we envision that the metasurfaces will play a significant role in the development of these technologies.

Online content

Any methods, additional references, Nature Research reporting summaries, source data, extended data, supplementary information, acknowledgements, peer review information; details of author contributions and competing interests; and statements of data and code availability are available at https://doi.org/10.1038/s41566-019-0536-x.

Received: 22 March 2019; Accepted: 13 September 2019;
Published online: 28 October 2019

References

1. Zernike, F. How I discovered phase contrast. *Science* **121**, 345–349 (1955).
2. Lang, W. *Nomarski Differential Interference-Contrast Microscopy* (Carl Zeiss, 1982).
3. Popescu, G. *Quantitative Phase Imaging of Cells and Tissues* (McGraw Hill, 2011).
4. Park, Y., Depeursinge, C. & Popescu, G. Quantitative phase imaging in biomedicine. *Nat. Photon.* **12**, 578–589 (2018).
5. Alford, R. et al. Toxicity of organic fluorophores used in molecular imaging: literature review. *Mol. Imaging* **8**, 341–354 (2009).
6. Lee, K. et al. Quantitative phase imaging techniques for the study of cell pathophysiology: from principles to applications. *Sensors* **13**, 4170–4191 (2013).
7. Marquet, P. et al. Digital holographic microscopy: a noninvasive contrast imaging technique allowing quantitative visualization of living cells with subwavelength axial accuracy. *Opt. Lett.* **30**, 468–470 (2005).
8. Choi, W. et al. Tomographic phase microscopy. *Nat. Methods* **4**, 717–719 (2007).
9. Kim, T. et al. White-light diffraction tomography of unlabelled live cells. *Nat. Photon.* **8**, 256–263 (2014).
10. Zheng, G., Horstmeyer, R. & Yang, C. Wide-field, high-resolution Fourier ptychographic microscopy. *Nat. Photon.* **7**, 739–745 (2013).
11. Greenbaum, A. et al. Wide-field computational imaging of pathology slides using lens-free on-chip microscopy. *Sci. Transl. Med.* **6**, 267ra175 (2014).
12. Ghosh, K. K. et al. Miniaturized integration of a fluorescence microscope. *Nat. Methods* **8**, 871–878 (2011).
13. Helmchen, F., Fee, M. S., Tank, D. W. & Denk, W. A miniature head-mounted two-photon microscope: high-resolution brain imaging in freely moving animals. *Neuron* **31**, 903–912 (2001).
14. Ziv, Y. et al. Long-term dynamics of CA1 hippocampal place codes. *Nat. Neurosci.* **16**, 264–266 (2013).
15. Jahani, S. & Jacob, Z. All-dielectric metamaterials. *Nat. Nanotechnol.* **11**, 23–36 (2016).
16. Genevet, P., Capasso, F., Aieta, F., Khorasaninejad, M. & Devlin, R. Recent advances in planar optics: from plasmonic to dielectric metasurfaces. *Optica* **4**, 139–152 (2017).
17. Lalanne, P., Astilean, S., Chavel, P., Cambril, E. & Launois, H. Blazed binary subwavelength gratings with efficiencies larger than those of conventional échelette gratings. *Opt. Lett.* **23**, 1081–1083 (1998).
18. Lin, D., Fan, P., Hasman, E. & Brongersma, M. L. Dielectric gradient metasurface optical elements. *Science* **345**, 298–302 (2014).
19. Zhan, A. et al. Low-contrast dielectric metasurface optics. *ACS Photon.* **3**, 209–214 (2016).
20. Arbabi, A., Horie, Y., Bagheri, M. & Faraon, A. Dielectric metasurfaces for complete control of phase and polarization with subwavelength spatial resolution and high transmission. *Nat. Nanotechnol.* **10**, 937–943 (2015).
21. Arbabi, E., Arbabi, A., Kamali, S. M., Horie, Y. & Faraon, A. Controlling the sign of chromatic dispersion in diffractive optics with dielectric metasurfaces. *Optica* **4**, 625–632 (2017).
22. Chen, W. T. et al. A broadband achromatic metalens for focusing and imaging in the visible. *Nat. Nanotechnol.* **13**, 220–226 (2018).
23. Maguid, E. et al. Photonic spin-controlled multifunctional shared-aperture antenna array. *Science* **352**, 1202–1206 (2016).
24. Arbabi, E., Arbabi, A., Kamali, S. M., Horie, Y. & Faraon, A. Multiwavelength polarization-insensitive lenses based on dielectric metasurfaces with meta-molecules. *Optica* **3**, 628–633 (2016).
25. Kamali, S. M. et al. Angle-multiplexed metasurfaces: encoding independent wavefronts in a single metasurface under different illumination angles. *Phys. Rev. X* **7**, 041056 (2017).
26. Shi, Z. et al. Single-layer metasurface with controllable multiwavelength functions. *Nano Lett.* **7**, 041056 (2017).
27. Arbabi, E. et al. Two-photon microscopy with a double-wavelength metasurface objective lens. *Nano Lett.* **18**, 4943–4948 (2018).
28. Zhu, A. Y. et al. Compact aberration-corrected spectrometers in the visible using dispersion-tailored metasurfaces. *Adv. Opt. Mater.* **7**, 1801144 (2018).
29. Faraji-Dana., M. et al. Compact folded metasurface spectrometer. *Nat. Commun.* **9**, 4196 (2018).
30. Pahlevaninezhad, H. et al. Nano-optic endoscope for high-resolution optical coherence tomography in vivo. *Nat. Photon.* **12**, 540–547 (2018).
31. Arbabi, A. et al. Miniature optical planar camera based on a wide-angle metasurface doublet corrected for monochromatic aberrations. *Nat. Commun.* **7**, 13682 (2016).
32. Arbabi, A., Arbabi, E., Horie, Y., Kamali, S. M. & Faraon, A. Planar metasurface retroreflector. *Nat. Photon.* **11**, 415–420 (2017).
33. Avayu, O., Almeida, E., Prior, Y. & Ellenbogen, T. Composite functional metasurfaces for multispectral achromatic optics. *Nat. Commun.* **8**, 14992 (2017).
34. Zhou, Y. et al. Multilayer noninteracting dielectric metasurfaces for multiwavelength metaoptics. *Nano Lett.* **18**, 7529–7537 (2018).
35. Guo, C., Xiao, M., Minkov, M., Shi, Y. & Fan, S. Photonic crystal slab Laplace operator for image differentiation. *Optica* **5**, 251–256 (2018).
36. Kwon, H., Sounas, D., Cordaro, A., Polman, A. & Alù, A. Nonlocal metasurfaces for optical signal processing. *Phys. Rev. Lett.* **121**, 173004 (2018).
37. Huang, P. S. & Zhang, S. Fast three-step phase-shifting algorithm. *Appl. Opt.* **45**, 5086–5091 (2006).
38. Arbabi, E., Kamali, S. M., Arbabi, A. & Faraon, A. Full Stokes imaging polarimetry using dielectric metasurfaces. *ACS Photon.* **5**, 3132–3140 (2018).
39. Nguyen, T. H., Kandel, M. E., Rubessa, M., Wheeler, M. B. & Popescu, G. Gradient light interference microscopy for 3D imaging of unlabeled specimens. *Nat. Commun.* **8**, 210 (2017).
40. Wang, Z. et al. Spatial light interference microscopy (SLIM). *Opt. Express* **19**, 1016–1026 (2011).
41. Shaked, N. T. Quantitative phase microscopy of biological samples using a portable interferometer. *Opt. Lett.* **37**, 2016–2018 (2012).
42. Bon, P., Maucort, G., Wattellier, B. & Monneret, S. Quadriwave lateral shearing interferometry for quantitative phase microscopy of living cells. *Opt. Express* **17**, 13080–13094 (2009).
43. Baek, Y., Lee, K., Yoon, J., Kim, K. & Park, Y. White-light quantitative phase imaging unit. *Opt. Express* **24**, 9308–9315 (2016).
44. Bouchal, P. et al. Geometric-phase microscopy for quantitative phase imaging of isotropic, birefringent and space-variant polarization samples. *Sci. Rep.* **9**, 3608 (2019).
45. Paganin, D. & Nugent, K. A. Noninterferometric phase imaging with partially coherent light. *Phys. Rev. Lett.* **80**, 2586–2589 (1998).
46. Arbabi, E. et al. MEMS-tunable dielectric metasurface lens. *Nat. Commun.* **9**, 812 (2018).
47. Kamali, S. M., Arbabi, E., Arbabi, A., Horie, Y. & Faraon, A. Highly tunable elastic dielectric metasurface lenses. *Laser Photon. Rev.* **10**, 1002–1008 (2016).
48. She, A., Zhang, S., Shian, S., Clarke, D. & Capasso, F. Adaptive metalenses with simultaneous electrical control of focal length, astigmatism and shift. *Sci. Adv.* **4**, eaap9957 (2018).

Acknowledgements

This work was supported by the Caltech Innovation Initiative programe. The device nanofabrication was performed at the Kavli Nanoscience Institute at Caltech. We thank C. Choi and C. Yang for Fourier ptychography microscope measurements and helpful discussions. H.K. acknowledges a fellowship from Ilju organization.

Poděkování/financování

Author contributions

H.K. and A.F. conceived the project. H.K., E.A., S.M.K. and M.F.-D. designed and fabricated the samples. H.K. performed the simulations and measurements. H.K., E.A., S.M.K. and M.F. analysed the data. H.K., E.A. and A.F. co-wrote the manuscript. All authors discussed the results and commented on the manuscript.

Podíl/přispění autorů

Competing interests

H.K., E.A. and A.F. have submitted a patent application based on the idea presented in this work.

Patenty a duševní vlastnictví

Additional information

Supplementary information is available for this paper at https://doi.org/10.1038/s41566-019-0536-x.

Correspondence and requests for materials should be addressed to A.F.

Reprints and permissions information is available at www.nature.com/reprints.

Publisher's note Springer Nature remains neutral with regard to jurisdictional claims in published maps and institutional affiliations.

Odkaz na doplňkové informace

Citace

Nature styl

Article

8. Flühmann, C., Negnevitsky, V., Marinelli, M. & Home, J. P. Sequential modular position and momentum measurements of a trapped ion mechanical oscillator. *Phys. Rev. X* **8**, 021001 (2018).
9. Flühmann, C. et al. Encoding a qubit in a trapped-ion mechanical oscillator. *Nature* **566**, 513–517 (2019).
10. Waldherr, G. et al. Quantum error correction in a solid-state hybrid spin register. *Nature* **506**, 204–207 (2014).

Science styl

6. L. Nikolova, P. Ramanujam, *Polarization Holography* (Cambridge Univ. Press, 2009).
7. J. P. Balthasar *et al.*, Metasurface Polarization Optics: Independent Phase Control of Arbitrary Orthogonal States of Polarization. *Phys. Rev. Lett.* **118**, 113901 (2017). doi: 10.1103/PhysRevLett.118.113901; pmid: 28368630
8. A. Arbabi, Y. Horie, M. Bagheri, A. Faraon, Dielectric metasurfaces for complete control of phase and polarization with subwavelength spatial resolution and high transmission. *Nat. Nanotechnol.* **10**, 937–943 (2015). doi: 10.1038/nnano.2015.186; pmid: 26322944

ACS styl

Chemical Reviews

(423) Singh, P.; Singh, S. N.; Lal, M.; Husain, M. Temperature Dependence of *I*−*V* Characteristics and Performance Parameters of Silicon Solar Cell. *Sol. Energy Mater. Sol. Cells* **2008**, *92*, 1611−1616.
(424) Singh, T.; Öz, S.; Sasinska, A.; Frohnhoven, R.; Mathur, S.; Miyasaka, T. Sulfate-Assisted Interfacial Engineering for High Yield and Efficiency of Triple Cation Perovskite Solar Cells with Alkali-Doped TiO_2 Electron-Transporting Layers. *Adv. Funct. Mater.* **2018**, *28*, 1706287.

Jak sehnat článek/knihu, který/kterou potřebuji?

- **Legálně:** (Open Access, *arxiv.org* nebo přes univerzity a vědecká centra)

- **(ne)Legálně:** (články) *sci-hub.ru* a (knihy) *zlibrary.to/*

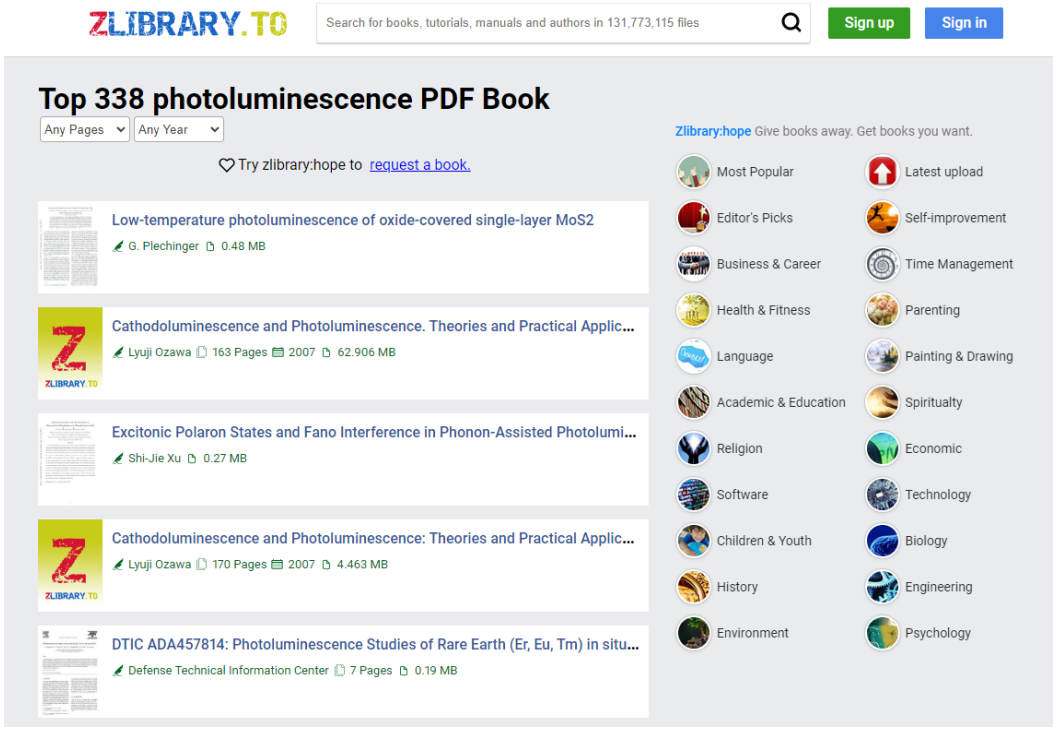

Nyní trocha filozofie…

Odstavec a věta

- mini-klíčová slova pro odstavce
- mikro-klíčová slova pro věty

Oslí můstek

Vhodné je položit fundamentální vědeckou **otázku** a v článku na ni naleznout **odpověď**

Text MIKROSKOPIE JE ZÁSADNÍ PRO text text text text text text text text text text text text text text text text text text text text text text text text text text text text text text text text text text text text text text text text text text text text text text text text text text text text text text text text text text text text text text text text text text text text text text text text text text text text text text BYL POUŽIT OBJEKVIT text text text text text text text text text text text text text text text text text text text text text text text text text text text text text text text text text text text text text text text text text text text text text text text text text text text text text text text text text text text text text text text text text text text text text text text text text text text text text text text text text text text text text text text POUŽITÍ TÉTO SESTAVY BYLO STĚŽEJNÍ PRO MĚŘENÍ VZORKU text text text text text text text text text text text text.

Text VZOREK BYL ZE SUPER-MATERIÁLU text.

Odstavec a věta

Nebezpečná místa!

První věta. Druhá věta. Třetí věta.

RESEARCH = [RE][SEARCH]
WRITING = [RE][WRITING]

改善

[KAI-ZEN]
[změna-dobro]

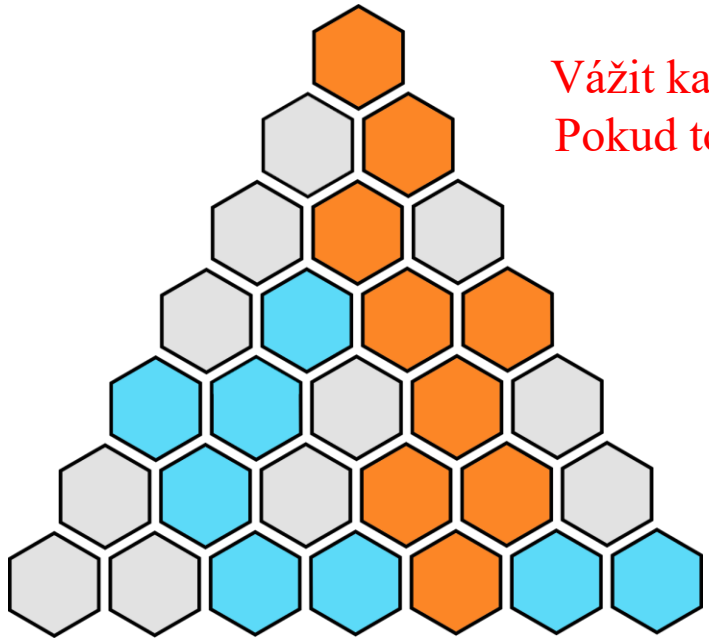

Vážit každou větu. (Není to protokol!)
Pokud to jde bez ní => pak ji nedávat.

Princip AZ kvízu
Úkolem je propojit všechny věty!

Na vše ostatní je tu Google a umělá inteligence…

„Jediným cílem při psaní článku je ho psát co nejjasněji a co nejjednodušeji pro čtení.“

„Neexistuje univerzální „správný způsob“ psaní, který by vyhovoval všem příběhům a za všech okolností.“

„Pamatujte: psaní je experimentální věda“

Věda > Psaní

K. W. Plaxco

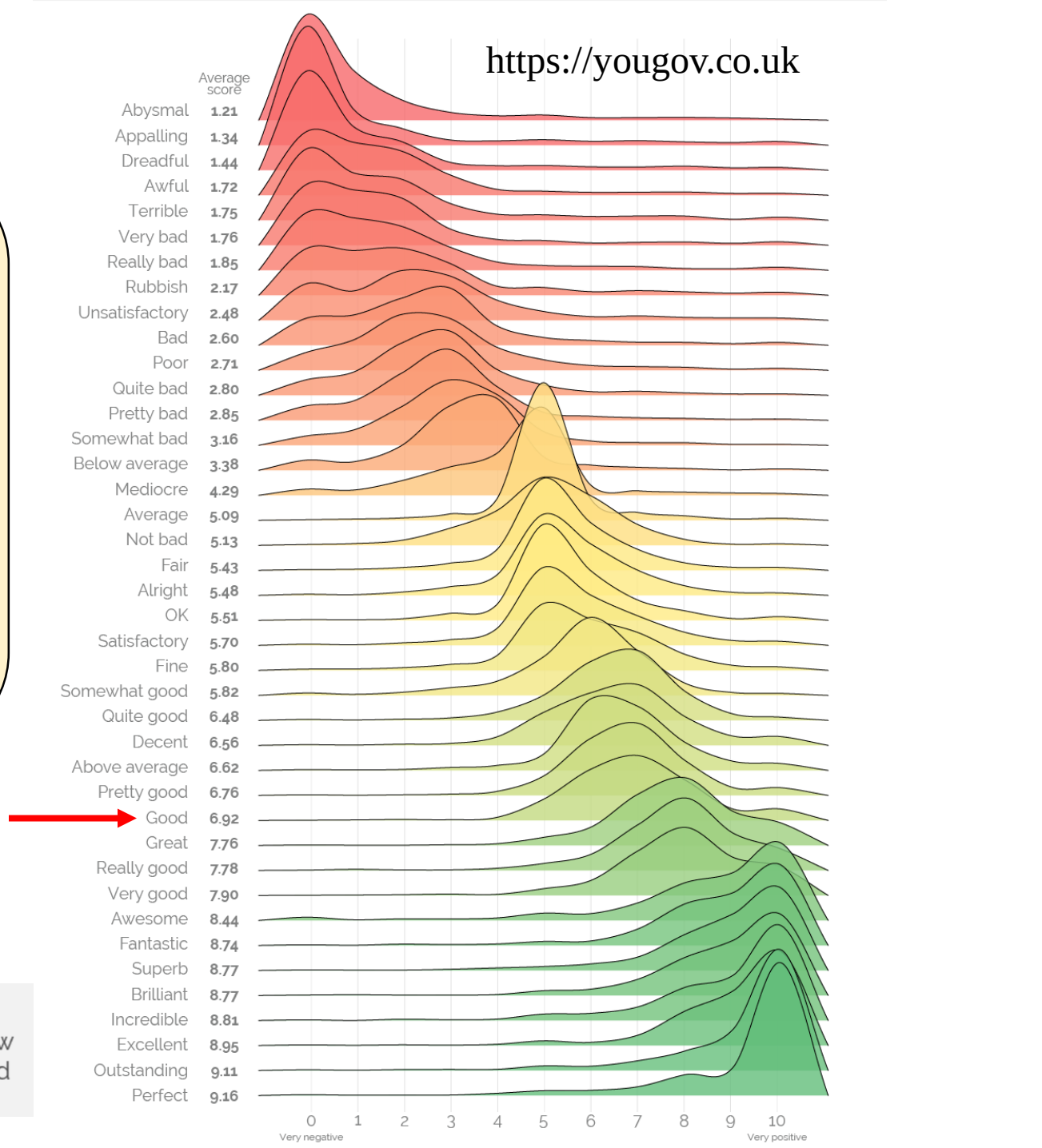

How good is "good"? Now with even more words!

On a scale of 0 to 10, where 0 is 'very negative' and 10 is 'very positive', in general, how positive or negative would the following word/phrase be to someone when you used it to describe something?

VYSOKÉ UČENÍ TECHNICKÉ V BRNĚ FAKULTA STROJNÍHO INŽENÝRSTVÍ

CEITEC
Central European Institute of Technology
BRNO | CZECH REPUBLIC

SOČ
středoškolská odborná činnost

Proč vlastně psát vědecké články?

krátká přestávka (5 min)

Ing. Petr Dvořák, Ph.D.
petr.dvorak@ceitec.vutbr.cz

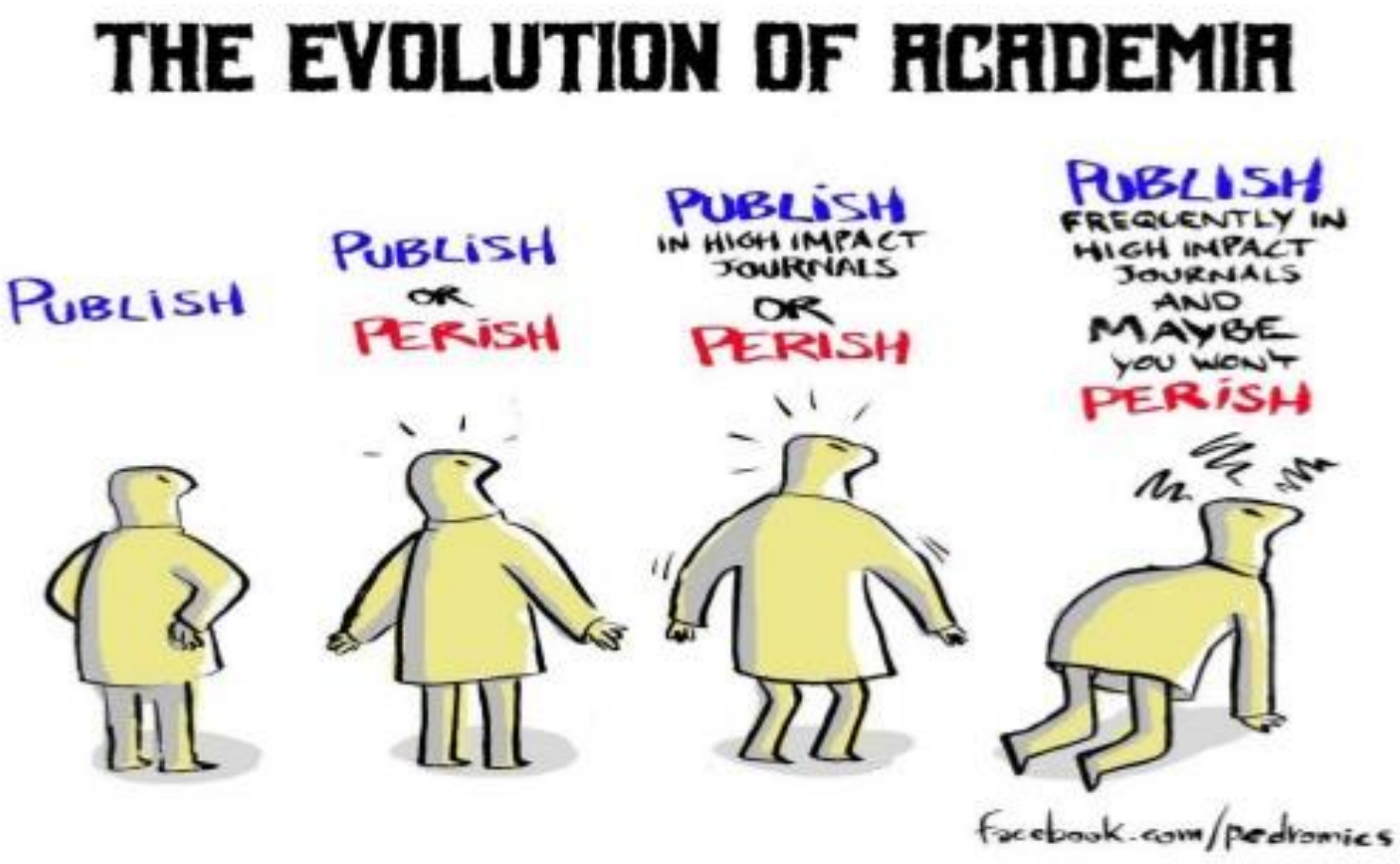

Peníze ve vědě

vs.

vědecká/věčná „sláva“

- Granty a indikátory projektů (závěrečné zprávy, mezníky, výstupy a požadavky grantů => **tlak na vědce**)
- Hodnocení vědy a „kafemlejnek“, hodnocení M17+
- Jak vybrat správný žurnál? (Q1, Q2, Q3 a Q4)
- Co to jsou predátorské časopisy?

VYSOKÉ UČENÍ TECHNICKÉ V BRNĚ FAKULTA STROJNÍHO INŽENÝRSTVÍ

CEITEC
Central European Institute of Technology
BRNO | CZECH REPUBLIC

SOČ
středoškolská odborná činnost

Jak probíhá recenzní řízení? (peer-review žurnály)

Ing. Petr Dvořák, Ph.D.

petr.dvorak@ceitec.vutbr.cz

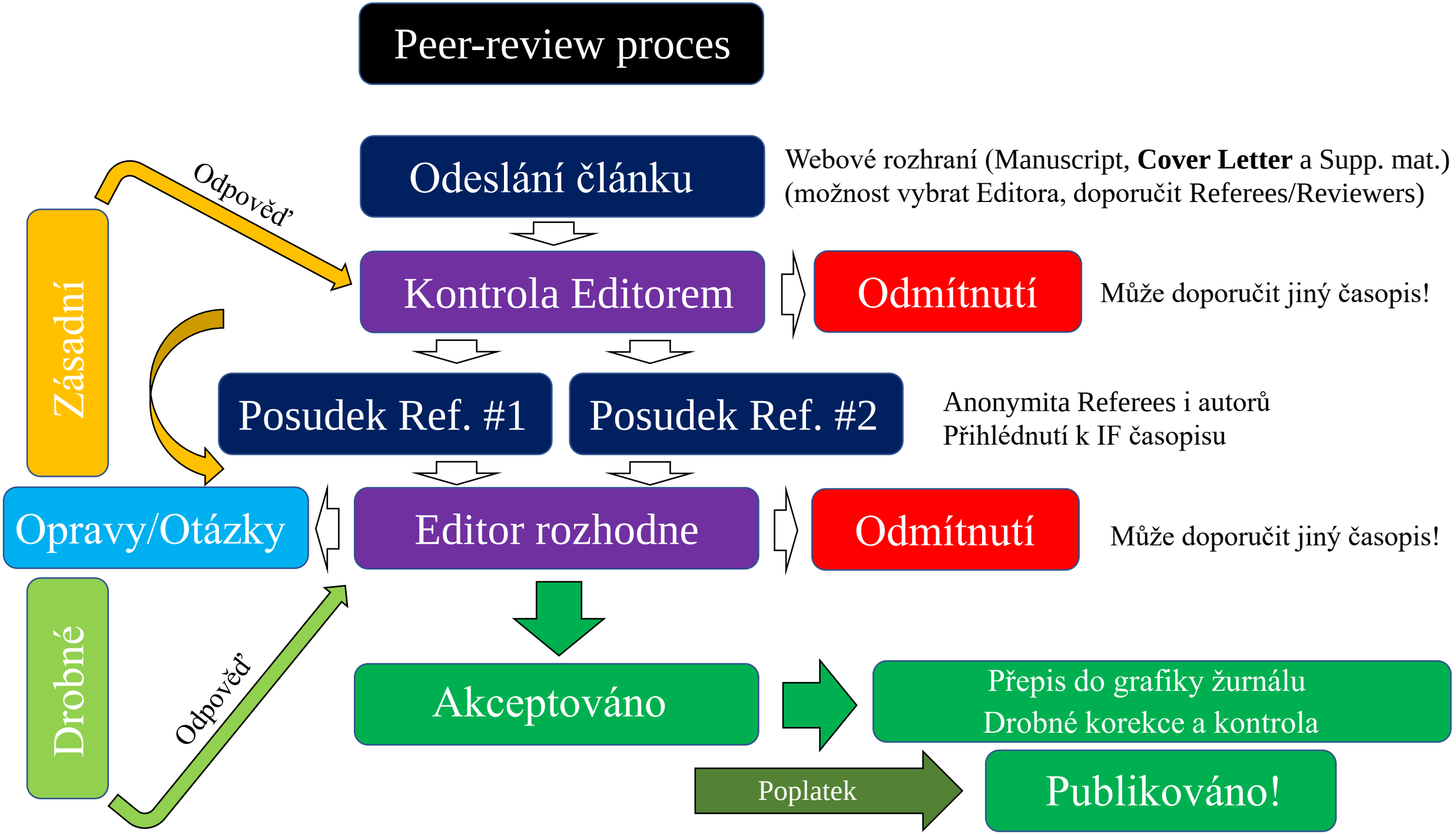
Peer-review proces
Odeslání článku
Webové rozhraní (Manuscript, **Cover Letter** a Supp. mat.)
(možnost vybrat Editora, doporučit Referees/Reviewers)
Odpověď
Zásadní
Kontrola Editorem
Odmítnutí
Může doporučit jiný časopis!
Posudek Ref. #1
Posudek Ref. #2
Anonymita Referees i autorů
Přihlédnutí k IF časopisu
Opravy/Otázky
Editor rozhodne
Odmítnutí
Může doporučit jiný časopis!
Drobné
Odpověď
Akceptováno
Přepis do grafiky žurnálu
Drobné korekce a kontrola
Poplatek
Publikováno!

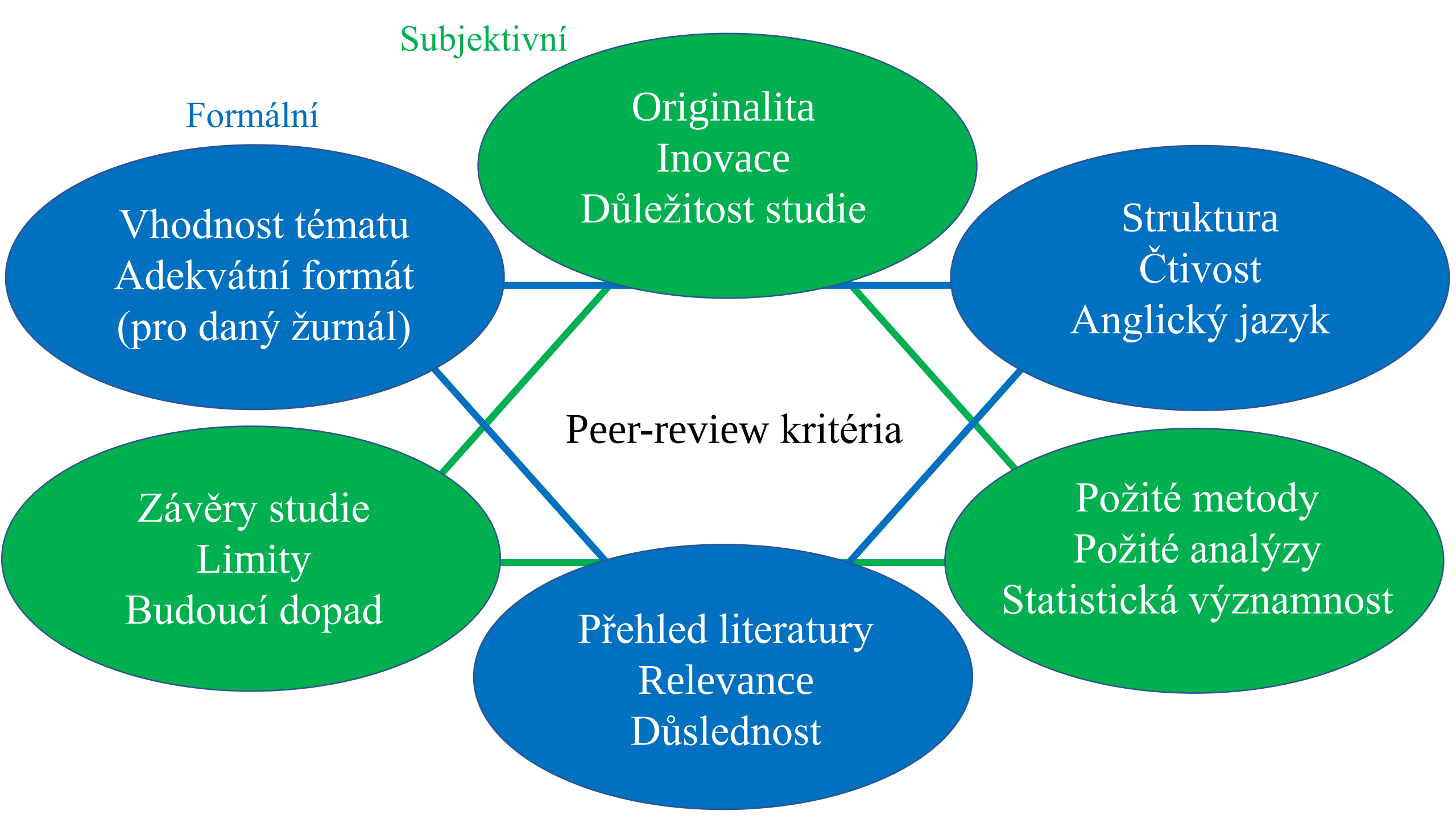
Subjektivní
Formální
Originalita
Inovace
Důležitost studie
Vhodnost tématu
Adekvátní formát
(pro daný žurnál)
Struktura
Čtivost
Anglický jazyk
Peer-review kritéria
Závěry studie
Limity
Budoucí dopad
Požité metody
Požité analýzy
Statistická významnost
Přehled literatury
Relevance
Důslednost

Cover Letter

Dr. Petr Bouchal
Central European Institute of Technology
Brno University of Technology
Brno, Czech Republic
Tel.: +420 54114 2759
E-mail: petr.bouchal@ceitec.vutbr.cz
Brno, November 26, 2018

Dear Editors of *Nano Letters*,

Please consider the enclosed manuscript, entitled **"High-resolution quantitative phase imaging of plasmonic metasurfaces with sensitivity down to a single nanoantenna"** for publication.

Metasurfaces are the new generation of optical components, which have already proven themselves capable of performing all sorts of both conventional and extraordinary optical functions. Ultrathin achromatic lenses, computer-generated holograms, quarter-wave plates, or polarimeters have been demonstrated, employing a variety of building blocks with subwavelength sizes. The key property of the great majority of these components is the spatial distribution of light phase they produce. Therefore, the tools that allow fast and reliable indication of phase response from individual nanoantennas are in great demand for rapid development and analysis of various metasurfaces.

In this submission, we demonstrate a new tool for instantaneous quantification of amplitude and phase of plasmonic metasurfaces providing unprecedented resolution and sensitivity, not achievable in state-of-the-art experiments. The measurement strategy is based on the principles of incoherent digital holographic microscopy, enhanced by optical elements controlling light through geometric (Pancharatnam-Berry) phase. In addition to the superior amplitude and phase sensitivity, our approach is inherently stable (common-path arrangement), and unique in combining high resolution and single-shot operation with guaranteed subnanometer precision and excellent accuracy. Although we demonstrated the capabilities of our method only using linear Pancharatnam-Berry metasurfaces, the measurement principle can be deployed also for analysis of nonlinear metasurfaces or metasurfaces based on the dynamic phase.

The optical performance and usability of the method was demonstrated by acquiring high-fidelity quantitative phase maps of a variety of metasurface structures, including vortex metalenses and vortex masks, nanoantenna arrays and metasurface gratings. In the first experiment of its kind, we demonstrated the widefield measurement of both amplitude and phase of light scattered by individual nanoantennas. The provided combination of high resolution and phase sensitivity with instantaneous operation is of great importance for study of fundamental effects and dynamics of phase variations in active metasurfaces, prototyping and characterizing of new building blocks, development of plasmonic biosensors or investigation of plasmonic-enhanced chirality.

The team working on this manuscript was composed of researchers who are especially experienced in the fields of phase imaging, singular optics and plasmonic metasurfaces, as demonstrated by our previous works, and our claims are all supported by the solid and clear evidence in the paper itself or in the supporting datasets. We believe that the scope (quantitative phase imaging of metasurfaces), major progress (excellent accuracy, high spatial and phase resolution, single nanoantenna sensitivity for the first time), high impact (real-time monitoring of metasurfaces) and novelty of our contribution will make it appropriate for *Nano Letters*.

On behalf of all co-authors,

Petr Bouchal

If you find the manuscript worthy of consideration for publication, we would like to suggest the following experts in the field as possible referees:

Thomas Zentgraf
University of Paderborn (Germany)
thomas.zentgraf@upb.de

Federico Capasso
Harvard university (USA)
capasso@seas.harvard.edu

Isabelle Staude
University of Jena (Germany)
isabelle.staude@uni-jena.de

Shuang Zhang
University of Birmingham (UK)
s.zhang@bham.ac.uk

Olivier Martin
EPFL, (Switzerland)
olivier.martin@epfl.ch

Rainer Hillenbrand
Nanogune, (Spain)
r.hillenbrand@nanogune.eu

VYSOKÉ UČENÍ TECHNICKÉ V BRNĚ FAKULTA STROJNÍHO INŽENÝRSTVÍ

CEITEC
Central European Institute of Technology
BRNO | CZECH REPUBLIC

SOČ
středoškolská odborná činnost

Jak psát **populárně**-vědecké články?

Ing. Petr Dvořák, Ph.D.
petr.dvorak@ceitec.vutbr.cz

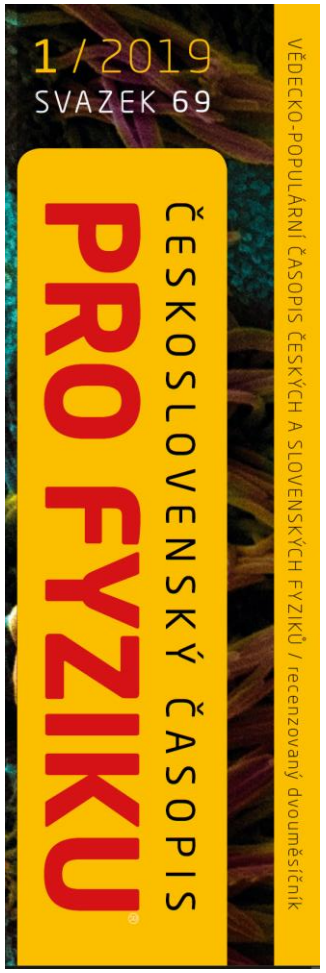

2D materiály aneb grafen a jak to bylo dál

Zdeňka Hájková[1], Martin Ledinský[1], Matěj Hývl[1], Aliaksei Vetushka[1], Antonín Fejfar[1], Jaroslava Řáhová[2], Otakar Frank[2]

[1] Fyzikální ústav AV ČR, v. v. i., Cukrovarnická 10/112, 162 00 Praha 6
[2] Ústav fyzikální chemie J. Heyrovského AV ČR, v. v. i., Dolejškova 2155/3, 182 23 Praha 8

Odlupováním vrstevnatých materiálů (např. grafitu) lze připravit 2D krystaly s tloušťkou jednoho nebo několika málo atomů. Nejznámějším takovým 2D materiálem je grafen (monovrstva grafitu), nicméně v současnosti existují a intenzivně se zkoumají desítky podobných struktur. Příspěvek podává základní přehled o 2D materiálech, jejich vlastnostech, metodách přípravy a možných aplikacích.

Začalo to grafenem

Existuje řada vrstevnatých materiálů, které mají silné kovalentní vazby mezi atomy vázanými ve vrstvě, zatímco jednotlivé vrstvy jsou k sobě poutány pouze slabými van der Waalsovými silami. Asi nejznámějším příkladem takovéhoto materiálu je grafit (tuha). Dlouhou dobu panovala názorová nejednotnost v tom, zda je možné oddělit jednotlivé vrstvy z těchto materiálů a připravit tak stabilní atomární 2D krystaly. Mnoho úsilí bylo věnováno pokusům o chemické či mechanické odlupování (exfoliaci), ale teprve roku 2004 André Geim a Konstantin Novoselov [1] popisem vlastností grafenu (monovrstvy grafitu) dokázali, že příprava dvojrozměrných materiálů není pouhou utopií.

Grafen je tvořen jednou vrstvou uhlíkových atomů uspořádaných hexagonálně, tedy ve vrcholech pravidelných šestiúhelníků (obr. 1c). Připraven byl nejprve z kousku grafitu metodou mechanické exfoliace (postupného oddělování stále tenčích a tenčích „vloček") pomocí běžné lepicí pásky. Tato velmi jednoduchá a rychlá metoda se stále používá ve výzkumu, protože umožňuje připravit vysoce kvalitní, byť velikostně značně omezený grafen. Velikost vloček takto připraveného grafenu bývá totiž typicky v řádu desítek až stovek mikrometrů, což je pro průmyslové uplatnění při výrobě obrazovek či displejů opravdu málo. Pro výrobu větších ploch grafenu se dnes využívá jiných metod, zejména depozice z plynné fáze (CVD – *Chemical Vapour Deposition*), kdy grafen narůstá za vysokých teplot ze směsi par methanu a vodíku na povrchu katalytického kovu (obvykle mědi či niklu). Tato metoda sice umožňuje připravit velké plochy grafenu, ale již při samotném růstu vzniká řada nedokonalostí v grafenové síti (hranice různě orientovaných zrn, oblasti s dvojvrstvou apod.) Navíc je třeba grafen z kovu přenést na jiný substrát (křemík, SiO_2, Al_2O_3 apod.) a právě transfer způsobuje vznik dalších defektů grafenu (vznikají trhlinky a tzv. vrásky, povrch bývá kontaminován polymerem používaným jako podpůrná vrstva při transferu či nedokonale opláchnutým roztokem sloužícím k odstranění kovu atp.) [2].

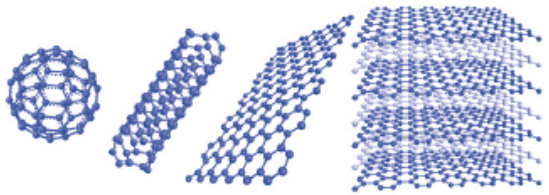

Obr. 1 Uhlíkové alotropy s různou rozměrovostí: (a) fulleren (0D), (b) uhlíková nanotrubička (1D), (c) grafen (2D), (d) grafit (3D). *Převzato z [4].*

Čím jsou 2D materiály zvláštní? Mají jiné vlastnosti než 3D materiály stejného chemického složení!

Rozměrovost je velmi důležitým parametrem, který ovlivňuje vlastnosti daného materiálu. Materiály mající stejné chemické složení mohou mít značně odlišné vlastnosti v závislosti na tom, jaké jsou jejich rozměry. Podíváme-li se např. na uhlíkové materiály s hybridizací sp^2 (obr. 1), pak kulovité molekuly (0D) tvořené desítkami uhlíkových atomů jsou známy jako fullereny, zatímco jsou-li fullereny v jednom směru významně protažené (1D), jedná se o uhlíkové nanotrubičky. Na grafen (2D síť uhlíkových atomů) se lze dívat jako na rozbalenou uhlíkovou nanotrubičku nebo jako na jednu vrstvu z grafitu (3D materiál) [3]. Vlastnosti jednotlivých modifikací uhlíku se od sebe významně liší, a to již na první pohled. Zatímco grafit je šedá, kovově lesklá, měkká a křehká pevná látka, grafen je prakticky průhledný (každá vrstva absorbuje jen 2,3 % světla), elastický a patří k nejpevnějším známým materiálům vůbec. Kromě toho je grafen také výborně elektricky a tepelně vodivý (je dokonce lepším vodičem

- Jednoduché „Review"
- Využívat odborné „Review"
- Vhodný historický kontext
- Přehledové citace (jen pár)
- Výukově a zajímavosti
- Hypotetické aplikace

Ve zkratce

Krásy plazmoniky: ŠÍŘENÍ A INTERFERENCE SVĚTLA NA POVRCHU KOVOVÝCH NANOSTRUKTUR

Radek Kalousek, Petr Dvořák, Jiří Spousta, Tomáš Šikola

Ústav fyzikálního inženýrství, Fakulta strojního inženýrství Vysokého učení technického v Brně, Technická 2, 616 69 Brno
CEITEC VUT, Vysoké učení technické v Brně, Purkyňova 123, 612 00 Brno

Co je plazmonika?

Tato oblast fyziky zkoumá, jak může být vybuzeno a detekováno světlo (tj. elektromagnetické pole) omezené na oblast o rozměrech významně menších, než je jeho vlnová délka. Tedy například to znamená, že se zabývá možnostmi jak zlepšit rozlišení optických prvků pod difrakční limit známý z vlnové optiky. Jedním ze způsobů jak excitovat takové světlo, je využití interakce elektromagnetického pole s volnými nosiči náboje ve vodivých tenkých vrstvách nebo ve vodivých nanostrukturách, tj. v objektech majících alespoň jeden rozměr menší než 100 nm. Plazmonika, která spojuje optiku a fyziku pevných látek, tedy úzce souvisí s rozvojem nanotechnologií, a proto tento moderní obor začíná psát svoji historii teprve zhruba na konci 20. století. Ucelené pojednání o základech plazmoniky a jejích aplikacích je např. v [1], o nejnovějších trendech v plazmonice se lze pak dočíst např. v [2].

Elektromagnetická vlna ve vodiči představuje elektromagnetické pole svázané s kmity nábojové hustoty volných nosičů náboje, jejichž kvantum se nazývá *plazmon*. A právě od názvu této kvazičástice se odvozuje název *plazmonika*. Lze tedy říci, že ve vodiči tak existuje smíšené pole, jehož energie má jak složku mechanickou, spojenou s plazmovými kmity, tak elektromagnetickou, spojenou s elektromagnetickým polem. Kvantum tohoto smíšeného pole se nazývá *plazmonový polariton*.

Potřebná teorie, která byla později v plazmonice využívána, byla rozvíjena již od počátku 20. století. Například v telegrafii byl řešen problém šíření elektromagnetických evanescentních (tento pojem bude vysvětlen dále) radiových vln *Jonathanem Zenneckem* [3] a *Arnoldem Sommerfeldem* [4]. V průběhu několika dalších desetiletí byly zaznamenány významné pokroky v mikrotechnologiích, později nanotechnologiích, a subtilní plazmonické jevy mohly být i experimentálně zkoumány. Excitace plazmonů v kovových tenkých fóliích byla poprvé pozorována pomocí spektroskopie energiové ztráty elektronů (EELS – z angl. *Electron-Energy Loss Spectroscopy*) již ve 40. letech [5]. O 20 let později byla provedena podobná měření, tentokrát byl studován vliv míry zoxidování povrchu na energiové ztráty elektronů. Ukázalo se, že kromě excitace plazmonů uvnitř kovového materiálu vzniká další energiová ztráta, a to v důsledku oscilací elektronového plynu na kovovém povrchu [6]. Právě s tímto typem kmitů souvisí evanescentní elektromagnetická vlna na rozhraní kov–dielektrikum popsaná Zenneckem a Sommerfeldem. Kvantu příslušného smíšeného foton-plazmonového pole, jehož energie se šíří podél rozhraní, se začalo říkat povrchový plazmonový polariton [7]. Amplituda kmitů elektrické a magnetické intenzity zde klesá se vzdáleností od rozhraní na obou jeho stranách (odtud název evanescentní, z lat. *evanescere* – vymizet, zaniknout), což znamená, že energie evanescentních vln se přenáší pouze v úzké oblasti podél rozhraní. Tato oblast je menší, než je vlnová délka použitého světla, a tudíž tento typ elektromagnetického pole je pro plazmoniku předmětem zkoumání.

Ústředním pojmem tohoto příspěvku jsou především *evanescentní vlny*. V dalším se proto zaměříme na jejich fyzikální podstatu, vznik, šíření a detekci. Dále popíšeme, jak lze připravit vzorky, na kterých je možné tyto vlny pozorovat, a jakou techniku je třeba k tomu použít. Na závěr ukážeme interferenci dvou evanescentních vln šířících se proti sobě.

Plazmonika představuje slibnou oblast pro rychlý přenos informace v integrovaných obvodech využívajících elektromagnetické pole o vysokých frekvencích.

Závěrem…

- Uspokojivý pocit
- Utřídíte si své myšlenky (vymyslíte si budoucí kroky)
- (Konečně) zpracujete své výsledky a data
- Ostatní Vám mohou říct svůj názor a poradit
- S každým publikovaným článkem se vám bude lépe psát další

- Princip vědy a pokroku:

Začít tam, kam došli ostatní před vámi

Děkuji za pozornost!

Reference:

- Glasman-Deal, H.: *Science Research Writing For Non-Native Speakers of English*, Icp illustrated edition, (2009)
- Bradac, C.:*An Educated Guide To Scientific Writing*, CreateSpace Independent Publishing Platform, (2018)
- Plaxco, K. W.: *The Art of Writing Science*, Protein Science, (2010)
- Rougier, N. P., Droettboom, M., Bourne, P. E.: *Ten Simple Rules for Better Figures*, PLOS, (2014)
- Tufte, E. R.: *The Visual Display of Quantitative Information*, Graphics Press, (2001)
- Doumont, J.-L.: *Trees, Maps, and Theorems Effective Communication for Rational Minds*, Principiae, (2009)

VYSOKÉ UČENÍ TECHNICKÉ V BRNĚ FAKULTA STROJNÍHO INŽENÝRSTVÍ

CEITEC
Central European Institute of Technology
BRNO | CZECH REPUBLIC

SOČ
středoškolská odborná činnost

Jak psát závěrečné práce?
aneb
bakalářské, diplomové a disertační práce

Pro zájemce pokud zbyde čas

Ing. Petr Dvořák, Ph.D.
petr.dvorak@ceitec.vutbr.cz